Northern Ocean Rapid Surface Evolution (NORSE): Science and Experiment Plan

Megan Ballard[1], Jennifer MacKinnon[2], Luc Rainville[3], Harper Simmons[4], Phil Abbot[11], Kerstin Bergentz[2], Ailin Brakstad[12], Luca Centurioni[2], John Colosi[7,8], Tim Duda[5], Tom Farrar[5], Ilker Fer[12], Laur Ferris[9], Donglai Gong[9], Verena Hormann[2], Steven Jayne[5], Leah Johnson[3], Craig Lee[3], Drew Lucas[2], Sophia Merrifield[2], Derek Olson[7], Pierre-Marie Poulain[10], Vince Premus[11], D. Benjamin Reeder[7], Edward Richards[8], Angel Ruiz-Angulo[13], Jason Sagers[1], Roger Samelson[6], Alejandra Sanchez-Rios[2], Anna Savage[2], Justin Shapiro[3], Eric Skyllingstad[6], Thomas Spengler[12], Jim Thomson[3], Kjetil Våge[12], and Kristin Zeiden[3]

[1] Applied Research Laboratories at the University of Texas at Austin
[2] Scripps Institution of Oceanography, University of California San Diego
[3] Applied Physics Laboratory and School of Oceanography, University of Washington
[4] College of Fisheries and Ocean Sciences, University of Alaska Fairbanks
[5] Woods Hole Oceanographic Institution
[6] Oregon State University
[7] Naval Postgraduate School
[8] University of California Santa Cruz
[9] Virginia Institute of Marine Science
[10] Centre for Maritime Research and Experimentation, NATO
[11] Ocean Acoustical Services and Instrumentation Systems
[12] University of Bergen
[13] University of Iceland

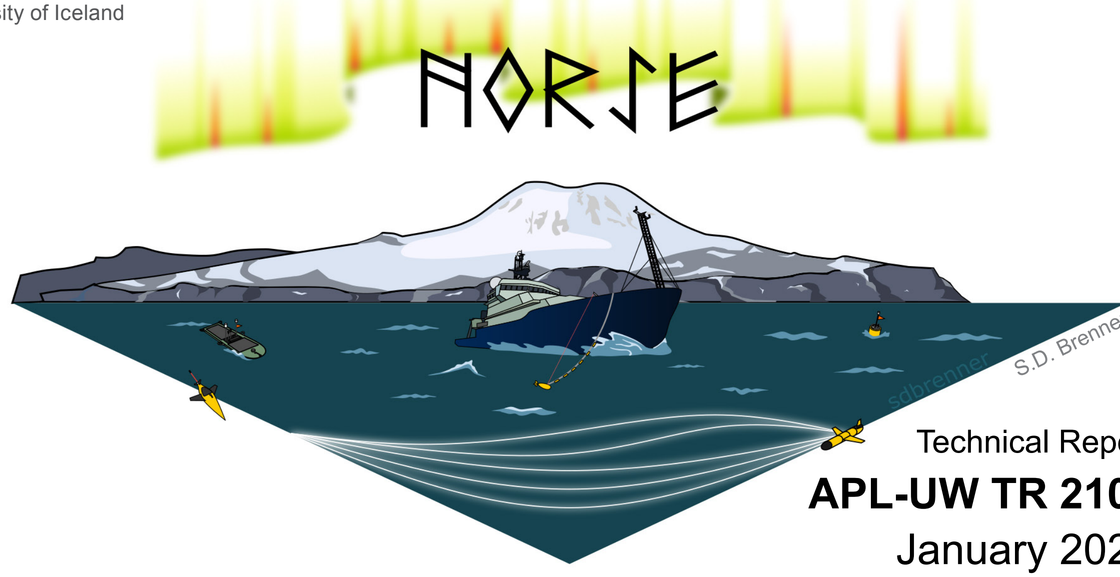

Technical Report
APL-UW TR 2102
January 2022

Applied Physics Laboratory University of Washington
1013 NE 40th Street Seattle, Washington 98105-6698

Grants: N00014-21-1-2768 (Rainville, Johnson, Lee); N00014-21-1-2739 (Savage, MacKinnon); N00014-21-1-2717 (Simmons, Shapiro); N00014-21-1-2743 (Thomson, Zeiden); N00014-21-1-2742 (Centurioni, Hormann); N00014-21-1-2745 (Farrar); N00014-21-1-2741 (Lucas); N00014-21-1-2701 (Gong); N00014-21-1-2738 (Jayne); N00014-21-1-2740 (Samelson, Skyllingstad); N00014-21-1-2744 (Poulain); N00014-21-1-2919 (Ballard, Sagers)

CONTENTS

This page intentionally blank.

1. Introduction

From a top-down perspective, the upper ocean is an integrator of atmospheric forcing, where fluctuations in heat and salinity are usually attenuated compared to the time and space scales of freshwater and heat anomalies (and flux patterns) at the surface. This notion, that atmospheric forcing sets the spatial and temporal scales of upper ocean variability, is challenged by the existence of dynamically important lateral density structure across a range of scales in the upper ocean. This heterogeneous density field interacts with boundary layer turbulence in unique ways such that a spatially uniform surface forcing generates non-uniform mixing across the upper ocean (e.g., *Hosegood et al*., 2006; *Swart et al*., 2020; *Damerell et al*., 2020).

Instabilities associated with strong lateral density gradients and shear can drive rapid changes in upper ocean structure, producing variability in temperature, salinity, sound speed, and other properties at kilometer scales and modulating fluxes of momentum, buoyancy, and heat (*Skyllingstad and Samelson*, 2012; *Thompson et al*., 2016; *Skyllingstad et al*., 2017; *du Plessis et al*., 2019). At subpolar latitudes, where atmospheric forcing can be extreme and the internal deformation radius is small, these processes unfold at short lateral scales (small mesoscale to submesoscale, tens to ones of km) and temporal scales (hours to days), making them difficult to observe and to capture in regional-scale models. Understanding the characteristics of this temporal and spatial variability in the target region is a goal of this project.

Colosi and Rudnick (2021) report that ocean mixed layer and transition layer sound speed structure can produce significant variations in acoustic transmission loss at mid- and low frequencies. They hypothesize that these variations result from a combination of upper ocean structure imposed by distinct mesoscale and submesoscale upper ocean features, such as eddies, filaments and fronts, and stochastic structures associated with phenomena such as internal waves and small-scale thermohaline variability. The faster time scales associated with submesoscale processes at higher latitudes, and shallow acoustic ducting created by the vertical temperature structure of the Nordic Seas make acoustic propagation paths and transmission losses in regions north of Iceland particularly sensitive to upper ocean forcing events (Fig. 1).

The Nordic Seas northeast of Iceland provide an excellent example of the targeted physics. Warm saline waters carried by the Norwegian Atlantic Current mix with cooler and fresher waters within the Lofoten Basin, Norwegian Sea Gyre, and East Greenland Current (Fig. 2), producing complex thermohaline variability. The different water masses are stirred and stretched into small fronts by persistent mesoscale circulations (*Raj et al*., 2016). The sharp fronts distributed through the basin and along the edge of the mesoscale eddies rapidly evolve through interaction and competition with the turbulent background environment.

The Northern Ocean Rapid Surface Evolution (NORSE) Departmental Research Initiative (DRI) focuses on characterizing the key physical parameters and processes that govern the predictability of upper-ocean rapid evolution events occurring in the ice-free high latitudes. The goal is to identify which observable parameters are most influential in improving model predictability through inclusion by assimilation, and to field an autonomous observing network that optimizes sampling of high-priority fields. The objective is to demonstrate improvements in the predictability of the upper ocean physical fields associated with acoustic propagation over the course of the study. Broadly speaking, several processes are stochastic and ultimately require ensemble averages over possible ocean states, while others can be modeled and predicted.

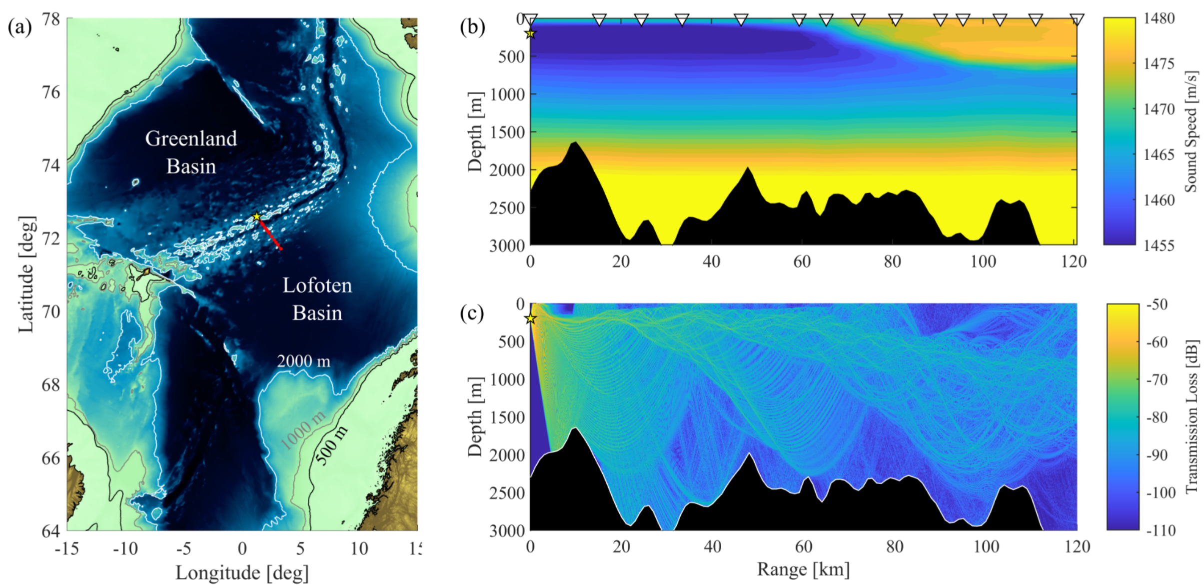

Figure 1. (a) Map showing the location of PROVOLO glider observations (*Bosse and Fer*, 2019a) with red dots marking the location of the profiles and yellow star marking the beginning of the transect. (b) Gridded sound speed from Mohns Ridge to the Lofoten Basin from PROVOLO glider with measurement locations indicated by the triangles. (c) Acoustic transmission loss calculated along the transect at a frequency of 1 kHz for a source depth of 200 m. The deepening of the subsurface duct as sound propagates across Mohns Ridge is evident.

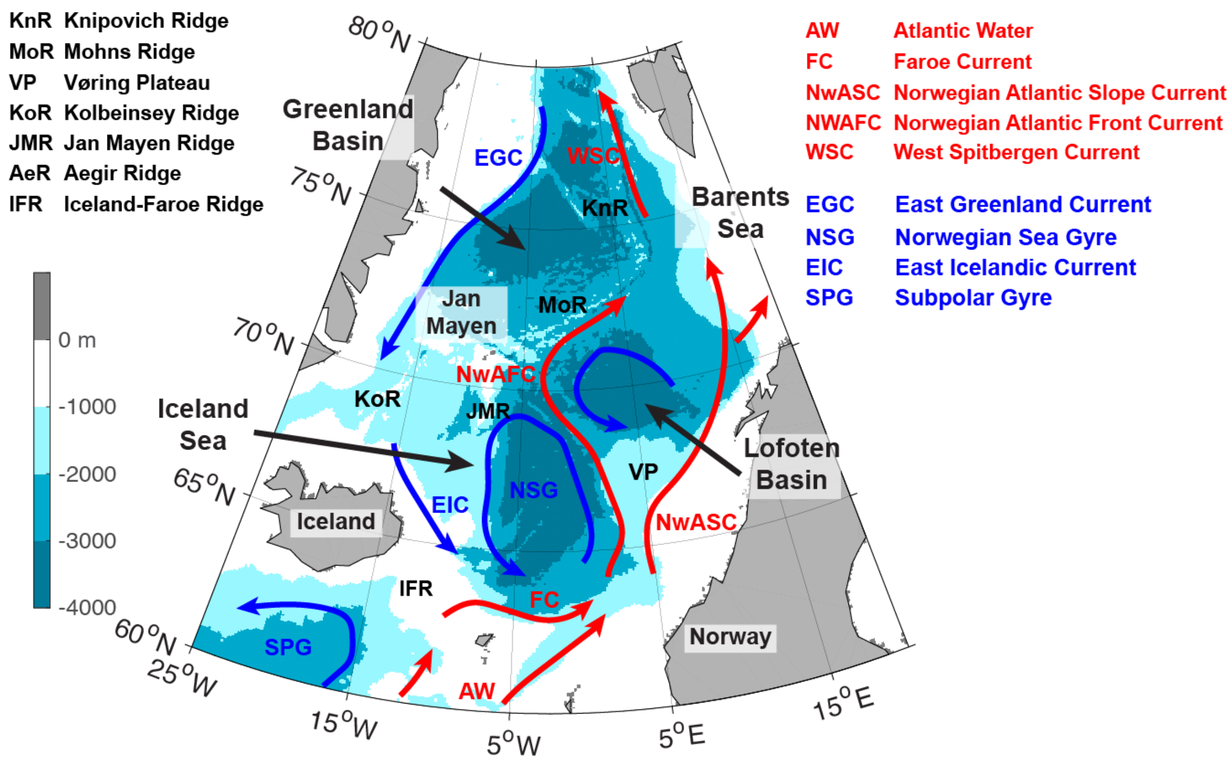

Figure 2. Map of the Nordic Seas, showing the bathymetry (background colors) and topographic features (with location names in black), and general upper ocean circulation of warm and salty Atlantic Water (current system labels and arrows in red) and cold fresh polar waters (in blue).

2. Background

Atmospheric forcing, mesoscale stirring, and numerous processes associated with lateral density contrasts drive upper ocean evolution across a range of spatial and temporal scales. An overview of the surface (Section 2.1) and stratified interior (Section 2.2) processes particularly relevant to acoustics (Section 2.3) are presented here.

2.1. Near-Surface Processes

The NORSE region is forced by both buoyancy and momentum (wind) fluxes. To model and predict variations in the sound propagation field accurately, the evolution of the surface boundary layer (SBL) deepening/shoaling, and turbulence within, needs to be predicted.

2.1.1. Surface Gravity Waves

Surface gravity waves and associated upper ocean processes such as wave breaking and Langmuir circulation Stokes drift are important for sound propagation, both through modification of the surface roughness and from the injection of bubbles. Bubbles cause increased acoustic transmission loss and are also a source of ambient sound. Further, surface wave breaking is known to elevate turbulent mixing well above the boundary layer scaling predictions (though only to depths of around one significant wave height). It is unclear how uneven distribution of bubble plumes and rain, and nonstationary surface roughness impact acoustic transmission loss. Furthermore, the fate of the scattered energy is an unresolved question — is it distributed diffusely throughout the water column, does it stay in the surface duct, or is it lost to transmission into the seafloor?

The winds and waves at the surface of the ocean are typically in a state of equilibrium, in which the steepness of the surface waves and the associated turbulence from wave breaking are set by the local wind stress (*Phillips*, 1985). This equilibrium is assumed in most forecast models, including empirical schemes that relate wind speed to the ambient noise field generated by breaking surface waves (*Wenz*, 1962). Figure 3 shows an example of wind–wave equilibrium, in which measured wave spectra match wind spectra and profiles of turbulent dissipation rate in the surface layer have an integral balance with the wind input rate (*Thomson et al*., 2013).

The wind–wave equilibrium can be disrupted, however, in conditions such as rapid evolution in winds, strong surface buoyancy fluxes, or wave–current interactions at fronts. All of these exceptions are common in the Nordic Seas, where storms pass rapidly, surface stratification due to the influence of arctic seasonal ice melt is strong, and mesoscale eddies are active. The lack of equilibrium causes canonical models for mixed layer depths (e.g., one-dimensional models like that of *Price et al*., 1986) and surface fluxes (e.g., COARE) to fail. These failings may, in turn, reduce the skill of acoustic propagation models. Furthermore, the generation of ambient noise by wave breaking will be altered from wind based climatology.

2.1.2. Sloping Fronts

Strong mesoscale circulation stirs and strains the background temperature and salinity gradients to create a dynamic field of density fronts. Sloping fronts modulate all facets of SBL development including mean and local mixed layer depth, background stratification, upper ocean turbulence, and the remnant mixed layer. Theory, models, and observational process studies have identified specific dynamics occurring at sloping fronts, yet it is unclear how theoretical scalings (developed for idealized cases in a narrow parameter space) are useful in upper ocean prediction under surface forcing and in the presence of lateral variability due to the large parameter space in which different frontal processes exist. The influence of sloping fronts on the upper ocean differ in part based on the strength of the lateral density gradient, the depth of the mixed layer, and the surface forcing conditions that change within the Lofoten Basin throughout the year (Fig. 4).

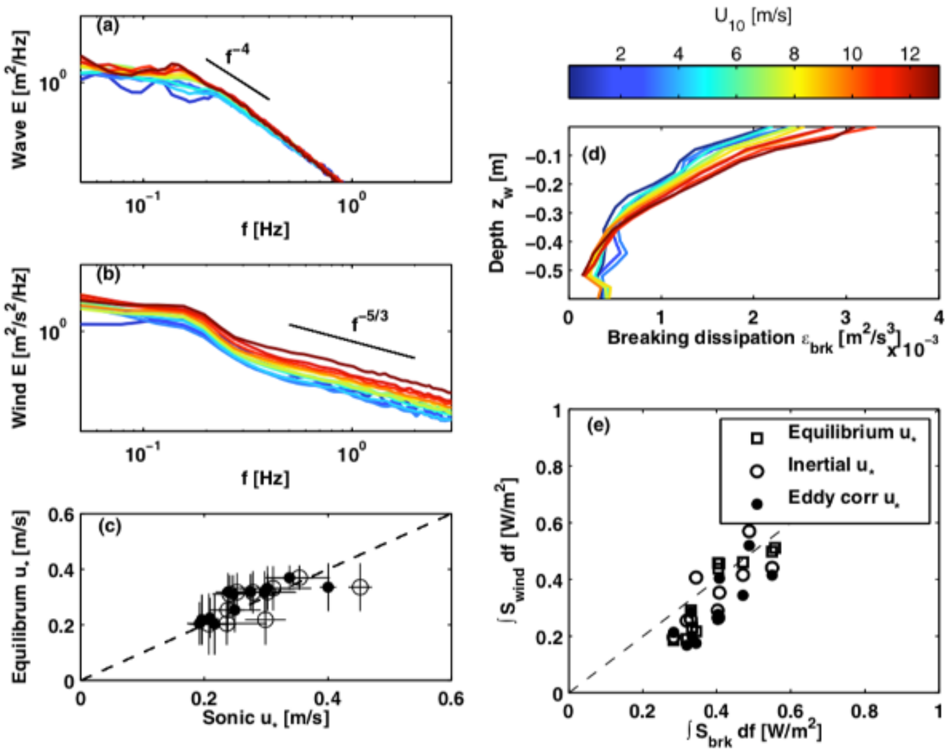

Figure 3. Example of wind–wave equilibrium over a range of conditions observed with SWIFT buoys: (a) wave spectra, (b) wind spectra, (c) wind friction velocity, (d) profiles of turbulent dissipation rate in the ocean surface layer, and (e) balance of wind input TKE flux with dissipation in the water. Reproduced from *Thomson et al*. (2013).

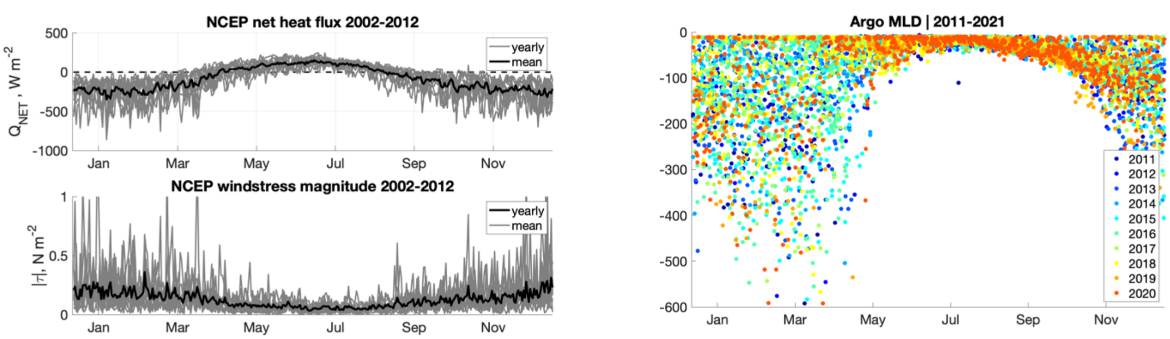

Figure 4. Left: Daily NCEP surface forcing at 70°N and 5°W from 2002–2012 (grey lines) and average of all years (black). Right: Mixed layer depths from Argo profiles collected at 60–70°N and –10–0°E from 2011–2021.

Winter storms cause deep mixing of hundreds of meters and incite waves that energize submesoscale flows (*Callies et al*., 2015). The interaction between mixing and quasi-balanced currents associated with near-surface fronts drive negative potential vorticity instabilities (*Thomas et al*., 2013) and diabatic and wave driven frontogenesis (*McWilliams et al*., 2015; *Bodner et al*., 2019; *Suzuki et al*., 2016). Fronts can also enhance surface wave breaking via wave–current interactions that modulate wave steepness. The deep mixed layers in turn increase available potential energy at sloped fronts, leading to baroclinic instability (*Fox-Kemper et al*., 2008) and pressure gradient imbalances (e.g., *Tandon and Garrett*, 1994; *Johnson et al*., 2020; *Pham and Sarkar*, 2018) that tilt the horizontal gradients into vertical stratification. The nonlinear interaction between all these processes under episodic forcing is poorly understood and leads to highly variable mixed layer depths in both space and time despite being subject to larger scale synoptic atmospheric events (Fig. 4). Additionally, turbulence–frontal interaction and accompanying instabilities drive strong ageostrophic circulations that inject tracer variability into the interior (*Spall*, 1995; *Thomas*, 2008). During the spring transition, the competition of these processes leaves an imprint on the upper ocean and within the remnant mixed layer (*Cole et al*., 2010). Throughout the summer, sloped fronts in shallow mixed layers develop strong submesoscale flows as the external strain field continues to stir background gradients, resulting in strong lateral variability in the very near-surface ocean. These near-surface fronts mediate the subduction of *spice variability* (temperature and salinity anomalies that have compensating effects on density but compounding effects on sound speed). Spice injected at the base of the SBL is subsequently stirred and mixed below (*Spiro Jaeger et al*., 2020), making an important but poorly understood contribution to upper ocean sound channels (*Colosi and Rudnick*, 2020; Section 2.2.4).

2.1.3. Near-Inertial Oscillations

Near-inertial oscillations (NIO) are ubiquitous in the surface ocean, particularly in areas of strong and episodic wind forcing. Wind driven NIO generation is often modeled as a one-dimensional process (e.g., *Pollard and Millard*, 1970), but it is becoming clear that lateral variations in near-surface vorticity, mixed layer depth, and mixed layer fronts may all have substantial roles in mediating how local winds resonantly or nearly resonantly force NIOs near the ocean surface (e.g., *Asselin et al*., 2020; *Thomas et al*., 2020). NIOs have been the primary focus of the NISKINe DRI, with analysis ongoing. NIOs are an important part of the momentum and energy budgets of the wind forced SBL, without which it is challenging to predict SBL deepening accurately. They are known to interact strongly with near-surface fronts in ways that influence both NIO evolution and frontal subduction, but are poorly understood. Preliminary work points to other properties of the background field such as gradients in velocity associated with NIOs being at times as important to acoustic propagation pathways and scattering as gradients in temperature and salinity, which are also poorly understood.

2.2. Stratified Ocean Processes

2.2.1. Large-Scale Fronts

The target region is home to several distinct water masses, delineated by strong fronts, the most prominent being the front between the Atlantic and Arctic waters between the Norwegian and Greenland seas. This front over Mohns Ridge supports a surface intensified baroclinic jet of 40 km width with geostrophic velocity exceeding 0.5 m/s (*Bosse and Fer*, 2019b). Temperature decreases by about 5°C across the front. Acoustic propagation pathways respond to both the average changes in sound speed properties across such water mass boundaries (see Fig. 1), and to the multiple timescales of variability associated with mesoscale frontal meandering and instabilities. While poorly sampled in situ, these fronts have signatures in surface dynamical heights and their structure can be well modeled and predicted (with the right initialization and boundary conditions).

2.2.2. Eddies

The Lofoten Basin is the most active eddy region in the Nordic Seas (*Raj et al*., 2020). These eddies detach from the Atlantic Slope Current and propagate southwest, and are also formed around the Atlantic Front Current. The Lofoten Vortex is a permanent anticyclonic eddy in the deepest part of the basin. Generally, anticyclonic eddies deepen the Atlantic Water (AW) while cyclonic eddies have the opposite effect. The drift speed of these eddies is about 5 km/day and they have a mean geometric radius of 16–22 km. Eddies modify acoustic propagation pathways in several ways: they are associated with sound speed gradients through sloping isopycnals that define the eddy, they are often associated with strong fronts on their edges that mediate subduction of spice and other water properties, they actively stir spice subsurface, and their strain and vorticity focus and trap propagating internal waves, sometimes leading to enhanced dissipation.

2.2.3. Internal Waves

Internal waves (IW) in the stratified ocean can be well represented by the Garrett–Munk (GM) spectral model, allowing them to be modeled as a stochastic process. This model has not been tested thoroughly at high latitudes. The GM model is not meant to represent internal waves near the ocean surface, particularly during and after strong forcing events. Furthermore, because of the prevalence of rough topography, locally generated internal tides (both high-mode internal tides near Mohns Ridge and lower-mode internal tides throughout this region) are likely to be important for modulating sound propagation. Internal tide generation and propagation is sensitive to (evolving) stratification and current structures near the ridge, and hence this signal is not entirely stationary.

2.2.4. Spice

Temperature/salinity variability (spice) created by variable atmospheric forcing is subducted/entrained at fronts and at the edges of eddies, creating spice anomalies in the stratified interior (*Spiro Jaeger et al*., 2020; *Sanchez-Rios et al*., 2020). This variability also has an important role in controlling the sound propagation and sound coherence. We expect that at some scales (10–20 km), spice anomalies can change sound speed by more than 5 m/s and refract sound both in the lateral and vertical directions (*Colosi and Rudnick*, 2020). We need to quantify the time and spatial scales associated with these anomalies as well as better understand the physical processes governing the entire life cycle (generation, subduction, stirring, and mixing/diffusion).

Some acoustic models (*Dushaw et al*., 2016) do not distinguish between sound speed fluctuation caused by IW isopycnal tilt and spice variations, which dually control the sound speed finestructure (*Dzieciuch et al*., 2004), but spice anomalies in unstratified mixed layers (which are inhospitable to IW propagation) dominate sound speed variability (*Rudnick*, 2004). *Bosse et al*. (2018) identified spiciness injection/removal by winter mixing in western Lofoten Basin, which contributes to double diffusive instability downstream to the north. AW is spicier than underlying waters that are cold and fresh (lower spice). Winter mixing (due to cooling and wind) creates mixing to 500 m depth, contributing spice to the underlying waters. The depth of mixing greatly affects the surface spiciness; mixing shallower than the AW salinity maximum reduces spice of near-surface waters by convective cooling and freshening (while mixing below the salinity maximum increases spice of deep waters), illustrating the potential effects of localized mixing events (e.g., storms) on spice anomalies.

2.2.5. Near-Inertial Waves

Near-inertial waves (internal waves near the inertial frequency) radiating downward into stratified waters have largely horizontal motions that do not cause large sound speed anomalies. However, when they have large shear the subsequent instabilities can result in mixing and sound speed profile adjustments. Observations show energetic packets of downward propagating near inertial (subintertial) waves trapped in the Lofoten Vortex, leading to elevated levels of turbulent mixing in the core of the eddy.

2.2.6. Turbulence and Mixing

Turbulent kinetic energy (TKE) dissipation provides the energy that homogenizes temperature and salinity gradients in the ocean, altering its structure. TKE is produced through a variety of physical processes. Wind stress (wind shear, breaking surface gravity waves, and Langmuir circulation) and meteorologically forced convection (cooling in this region) inject TKE into the SBL, mixing the upper ocean and transforming its density structure. The impact of atmospheric forcing events (storms) on mixing-induced stratification changes on both sides of fronts is of interest. A variety of mesoscale and submesoscale instabilities, especially near topographical and dynamical boundaries, mediate downscale energy cascade from the scales of forcing, eventually supplying energy to the turbulent microscale.

The horizontal structure of the Arctic Front is physically conducive to double diffusive instabilities and T-S intrusions that enhance lateral mixing. Baroclinic instability is known to act at the mesoscale in the Nordic Seas, but the role of smaller scale frontal instabilities in driving the forward energy cascade in the Norwegian Atlantic Front Current is unknown. Submesoscale overturning instabilities including symmetric (buoyancy/density gradient), gravitational (stratification), and centrifugal (vorticity) instabilities are most likely to develop sharp fronts. They can also be caused by the influence of topographic drag on vorticity. The boundary effects of the Jan Mayen and Mohns ridges may be conducive to the development of submesoscale overturning instabilities, which enhance vertical mixing. Strong internal wave generation over the ridges likely fuels wave–wave or wave–flow interactions, another source of TKE. The rich eddy field near the topographically complex Mohns Ridge may be favorable to internal wave–eddy interactions. With strong seasonal cycles in stratification and shear, the relative roles of turbulence producing physical processes should also exhibit a seasonal cycle.

2.3. Acoustic Propagation

Approaches to modeling acoustic propagation generally fall into two categories: deterministic (localized features such as fronts and eddies that lead to strong mode coupling or diffraction) and stochastic (random fields of internal waves and spice that cause acoustic scattering or scintillation). Deterministic techniques are applied to processes that may be measured directly or included in an ocean circulation model. Conversely, stochastic modeling approaches make use of the statistics of a process that may be characterized by measurements and represented by a model. The boundary between processes that one treats stochastically and deterministically can be fuzzy. For example, the mixed layer depth as a function of position and time can be treated either way depending on one's confidence in available information. The acoustic wavelength also has a role in dividing stochastic and deterministic features.

2.3.1. Mixed Layer Acoustic Duct

A mixed layer acoustic duct (MLAD) is usually associated with an upward refracting sound speed profile caused by the pressure gradient in a well-mixed layer. Ducted sound undergoes cylindrical spreading loss rather than spherical, and thus propagates further at usable strength. Furthermore, there is the question of the degree to which sound of a given frequency will be trapped within the MLAD or the AW secondary duct. Before the degree of trapping is addressed, we are initially interested in processes that affect sound pathways in a binary sense: the path exists or does not. Examples include duct appearance, disappearance, deepening, or large sound speed changes in the upper ocean that can affect critical depth and bottom interaction. Processes of interest here are ones that move fronts or significant features around, such as jets, frontal meanders, or eddy trajectories. Seasonality is important because there will be a surface duct in winter (incurring surface loss) and a subsurface duct in summer. The ability to know or to predict surface duct depth and geometry in detail is an interesting question that follows the binary existence question. The size and shape of a duct can have important consequences for sound propagation.

2.3.2. MLAD and Sound Channel Interactions Due to Scattering Processes

Second, if there is the potential for trapping, then there is the issue of diffractive and scattering induced interactions between the MLAD and the sound channel below, which can lead to MLAD energy loss as well as gain. Processes that affect the sound speed gradient at the boundaries of the duct, or, in other words, processes that generate and erode stratification, are likely to be variable in time and space and possibly intermittent in the study area. A few of the processes or features that perturb the depth of the duct and the gradient conditions beneath the duct (in the thermocline) are internal waves, fronts, eddies, and surface forcing.

2.3.3. Signal Randomization Due to Scattering Processes

Internal waves and small-scale spice are expected to generate stochastic short space and time scale variability in phase and transmission loss. This can be phrased as signal randomization leading to scintillation phenomena and loss of signal coherence. In general, this is due to processes that affect the details of the sound field, the temporal coherence behavior (coherence time scale), and coherence scales, which are always tied to phase structure functions and sometimes to intensity spatial scales (typical scales of a fade out or a glint region). In previous work focused on the main thermocline, the GM internal wave spectrum with stochastic propagation theories has been used with success to compare predictions to observations. In the upper ocean, where spice is equal if not dominant over internal waves in terms of sound speed variance, new approaches will likely be needed.

2.3.4. Surface Loss

Surface roughness scatters sound from one dominant ray or mode to others. Surface waves scatter sound and result in reflection loss each time sound is reflected from the surface. The specular reflection is weakened by transferring energy to other angles/modes, and some of the energy reflecting at high angles can be lost to the seabed. An open question is the degree to which the scattered energy can be ignored or must be accounted for. This question also depends on the observables being considered, such as acoustic intensity, scintillation, or coherence.

Reduced physics models, such as the transport theory developed by *Thorsos et al*. (2010) and used by *Raghukumar and Colosi* (2014), employ a perturbation approximation that accounts for both loss and redistribution of energy into other modes, and can provide estimates of coherence, but is only valid for small wave height compared to the acoustic wavelength. Reduced physics models that capture redistribution of acoustic energy and are transparent to the physical processes (such as sea surface roughness spectrum) for large sea surface roughness are at present out of reach. Numerical methods are available as well, such as 2D coupled mode theory (*Beilis* *and Tappert*, 1979), 3D coupled modes (*Ballard et al*., 2015), the 2D rough surface parabolic equation (*Rosenberg*, 1999), and 3D rough surface parabolic equations (*Lin*, 2019). In addition to the geometric effect included in these models, the bubble cloud from breaking waves causes attenuation due to viscous and thermal losses within the bubbles as well as scattering losses by re-radiation and a reduction in sound speed near the surface, which causes upward refraction and additional scattering loss (*Ainslie*, 2005).

2.3.5. Ambient Sound

Accurate characterization of ambient sound is critical to sonar performance prediction. The spectral level and directionality of ambient sound is a function of space and time, and it depends on both the sound generating mechanism as well as the propagation conditions. Ambient sound can be described in terms of the background spectral level as well as by transient sound events. The background level is attributed to a distributed collection of uncharacterized sources, commonly attributed to wind, waves, storms, and distant shipping. Bubbles are also an important source of ambient sound between 500 Hz and 50 kHz (*Wenz*, 1962). Transient sound sources include marine mammal vocalizations and nearby ships.

3. Science Objectives

The main objective of NORSE is to understand and develop knowledge on how *to predict the changes in acoustic propagation across ranges of less than 100 km*, *over time scales of a few days, particularly around times when the ocean changes rapidly* (e.g., storms). The governing questions include both those that are primarily physical oceanography questions and those that are primarily acoustics questions: **the crux of this experiment is the unique ability to look at how these physical oceanography and acoustics questions are intertwined and interdependent**.

The NORSE campaign will be guided by the following broad questions and the numerous implicit questions behind them. From a physical oceanography perspective, the following questions will be investigated:

1. During times of rapidly varying surface forcing, how well do one-dimensional models of mixed layer evolution agree with observations? To what extent are any discrepancies related to non-equilibrium surface wave states, near-inertial shear instability, or fundamental failure of stratified turbulence parameterizations in surface boundary layers (especially those that are either very shallow or very deep)?
2. To what extent does lateral variability in near-surface water properties on mesoscale, submesoscale, or sharp frontal scales influence how the ocean SBL responds to strong and variable forcing? Are there ways in which those scales of lateral variability feed back or imprint onto either the atmosphere or the stratified transition layer below?

3. How are temperature and salinity (and sound speed) characteristics in the stratified upper ocean influenced by the interplay between mesoscale eddies, stratified fronts, internal wave interaction with or trapping by either, subduction and mesoscale stirring of spice?

Each of the questions have implications for acoustic propagation. For every physical oceanography question, the following questions relate to its effects on acoustic propagation, including MLAD characteristics, diffraction, scattering, and surface loss:

4. What spatial and temporal information about the upper ocean structure is needed to predict the available acoustic propagation across an existing front or eddy? How accurate are state-of-the-art ocean sampling and assimilative modeling techniques at predicting acoustic path availability?
5. What are the spatial and temporal scales of phase and transmission loss for various sound paths propagating through a dynamically evolving ocean, e.g., across a front, eddy, or spatially inhomogeneous rain or wind event?
6. Are stochastic small scale processes like internal waves and spice important for determining acoustic path availability, and how do we measure upper ocean internal wave and spice models to predict this stochastic variability?

Measurements collected during NORSE will provide a better understanding of the coupled processes that drive rapid changes in the upper ocean at high latitudes, leveraging the adaptability and persistence of autonomous platforms.

4. Experiment Strategy

4.1. Observational Approach

4.1.1. NORSE Pilot Cruise

During the NORSE pilot cruise (September–October 2021) gliders, floats, SWIFTs, surface drifters, and Wave Gliders will characterize the environmental conditions across the acoustic propagation path, between a source deployed from the ship and a hydrophone array towed from a glider (Fig. 5). The mobile observing system will be used to identify regions that cause greatest uncertainty for acoustic transmission and collect key variables to predict the upper ocean evolution (and hence predict how acoustic transmission will change over time), reducing uncertainty. The NORSE pilot cruise will also assess the reliability and robustness of the Slocum G2/Towed Hydrophone Array system to the harsh conditions of the Norwegian Sea operating environment.

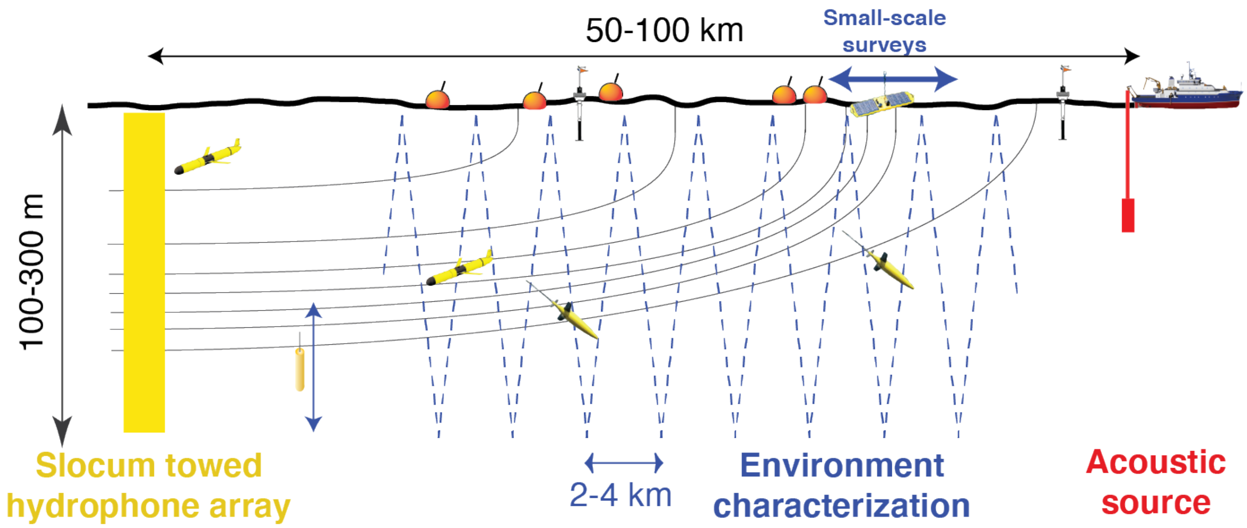

Figure 5. Schematic of the sampling strategies that will be used during the NORSE pilot cruise in September–October 2021.

Science Questions and Anticipated Outcomes

In addition to testing the reliability and robustness of equipment in the NORSE environment, measurements obtained from the NORSE pilot cruise will be used to address the following questions and refine sampling strategies for the yearlong NORSE experiment:

- Collect baseline measurements of transmission loss and ambient sound level in the NORSE environment
- Test our ability to predict sound propagation (transmission and travel time) given environmental measurements collected by the distributed autonomous systems
- Begin investigating surface loss models based on data from SWIFT drifters and other measurements of the air–sea interface dynamics

4.1.2. Geographically Fixed Ocean Observations

Deployment Strategy

A key component of NORSE will be the ability to obtain repeated observations of acoustic transmission across a well-characterized upper ocean environment for a complete annual cycle. A moored acoustic array will regularly transmit and receive across propagation distances of 30–50 km (see Section 5.2.1). Signals of 500–1500 Hz, sensitive to the processes outlined in Section 2, will be used.

The location of the mooring array is constrained by the geometry of the receiving array and considerations for yearlong survivability in high currents. The preference is to deploy the array at a depth less than 500 m with the recorder deployed on the seafloor. This will enable higher fidelity acoustic measurements by minimizing motion of the hydrophones. An attractive location is the shelf on the northern end of the Jan Mayen Ridge, either immediately east or south of Jan Mayen (Fig. 2). The region between Vøring Plateau and Jan Mayen and north along Mohns Ridge will be sampled during the pilot cruise.

The ocean between the acoustic source and receiving array will be characterized with several autonomous platforms. Underwater gliders will collect temperature and salinity to determine the location of fronts and how they evolve. More focused pilot and process studies (section 4.1.3), with a larger number of autonomous platforms and the ability to sample rapidly with shipboard instrumentation, will provide strategies to sample the important oceanic features during the multi-month deployments across the moored array. Additionally, the mooring lines will be instrumented with oceanographic sensors. These data sets will be used to reconstruct the sound speed profile along the acoustic propagation path and collect statistics of small scale processes for stochastic models. Measurements of atmospheric conditions, including wind speed, will also be collected. These data will be used to calculate surface loss and wind generated ambient sound.

In the current experiment concept, an acoustic source and receiving array will be deployed with a propagation path across the Jan Mayen Channel (JMCh) over a yearlong period. These mooring locations will monitor the acoustic response to the flow of water from the Greenland Sea to the Norwegian Seas through the JMCh (*Messias et al*., 2008; *Shao et al*., 2019). The dense waters from the Greenland Sea account for at least 20% of both the North Icelandic Jet and Faroe Bank Overflow (*Spall et al*., 2021). The volume of water exiting through the JMCh is estimated as 0.5–1.6 Sv (*Shao et al*., 2019; *Wang et al*., 2021). Previous measurements in the JMCh indicate that there is a steady deep flow from the Greenland Sea to the Norwegian Sea with an approximate velocity of 0.07–0.08 m/s (*Swift and Koltermann*, 1988; *Sælen*, 1990). However, the deep flow in the JMCh can reverse at times (*Østerhus and Gammelsrød*, 1999). In such cases, the JMCh is blocked and the water filling the channel has different distributions of water masses (*Wang et al*., 2021). The direction of flow in the JMCh is related to wind curl, and the flow through the JMCh is enhanced during periods of high North Atlantic Oscillation (*Köhl*, 2010).

The acoustic propagation from a source located on the north side of JMCh (6.3098°W, 71.2102°N) to a receiver array located near Jan Mayen Island (6.4422°W, 70.8448°N) is shown in Fig. 6. The sound speed profiles were constructed from shipboard CTD measurements collected in June 2015 (*Wang et al*., 2021). The sound speed profile in Fig. 6a is representative of the condition when the channel was blocked. In this case, the depth of the source at 100 m is above the sound speed duct resulting in sound that is initially downward refracted creating a conference zone propagation pattern. The impulse response contains arrivals that refracted in the duct. On the other hand, Fig. 6d shows a sound speed profile representative of Greenland Sea water flowing through the JMCh. The source is on the sound channel axis, resulting in sound that is trapped within the sound speed duct. This creates the high-amplitude finale in the impulse response (see Fig. 6f). This example demonstrates the sensitivity of the acoustic impulse response to the water mass present in the channel.

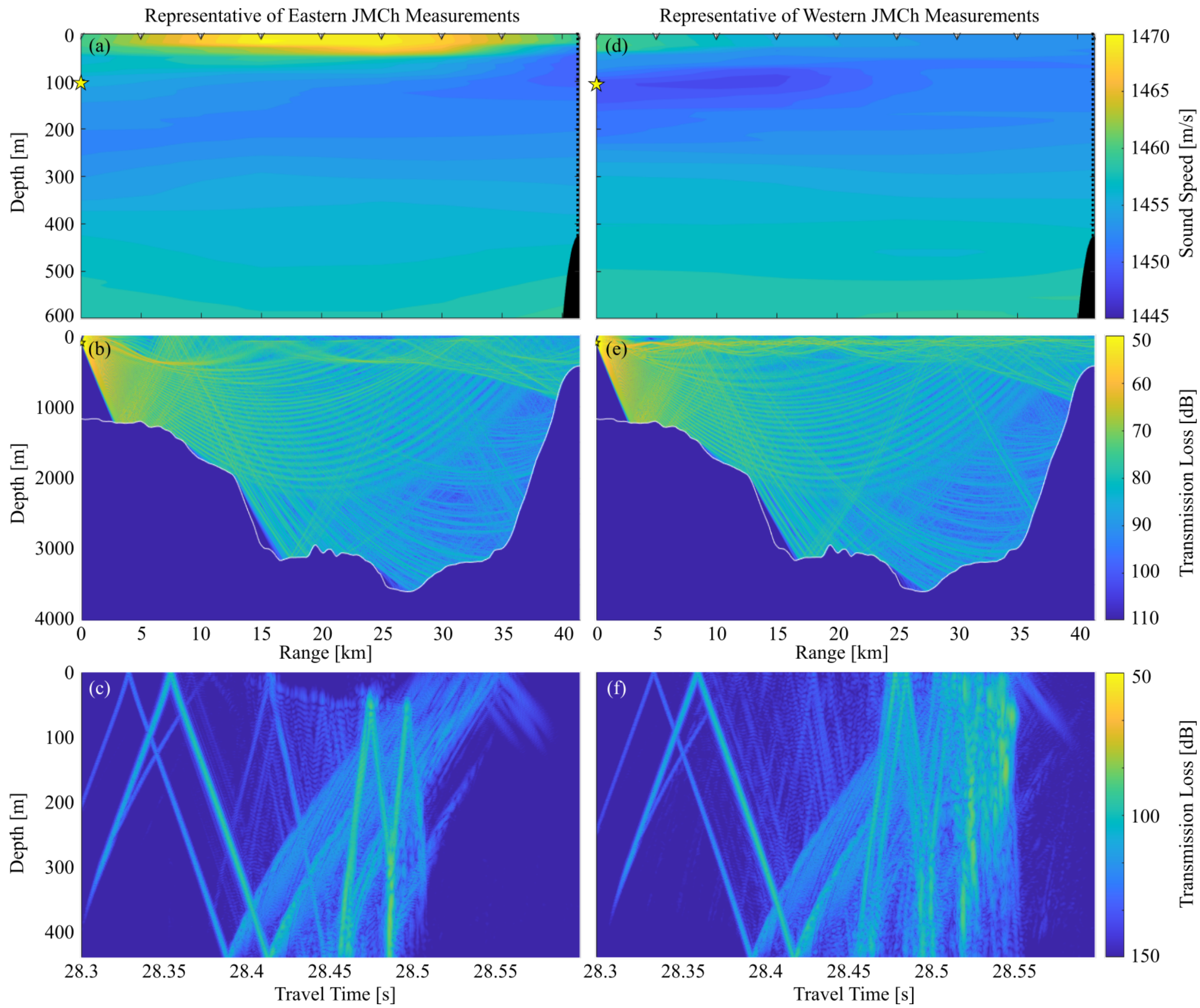

Figure 6. (a) Sound speed profiles constructed from CTD measurements shown in Fig. 7(c, f) from *Wang et al.* (2021) with the location of the acoustic source at 0 km to the location of the acoustic receiver array at 42 km. (b) Transmission loss for a 1-kHz source at a depth of 100 m. (c) Impulse response for measured by a vertical line array for a 1-kHz bandwidth centered at 1 kHz. (d–f) same as (a–c) except using CTD measurements shown in Fig. 7(d, g) from *Wang et al.* (2021).

The acoustic measurements from the moored source and receiver will take place over a yearlong period with transmission sets occurring every four hours. This sampling strategy will quantify variability on diurnal to seasonal scales.

Science Questions and Anticipated Outcomes

Measurements from the fixed acoustic source and receiver array will address the following research questions:

- What are the dominant oceanographic features affecting sound propagation in this environment? What acoustic metrics (transmission loss, travel time, coherence) are most affected by the environmental variabilities? How are these effects related to rapid surface evolution?
- How well can we predict acoustic propagation in this dynamic region? How well do ocean circulation models characterize the sound speed for acoustic propagation prediction in this environment? What features will be modeled deterministically versus stochastically?
- What are the effects of smaller scale features (i.e., internal waves and spice) on acoustic signal randomization and scattering? How do these processes affect scintillation phenomena and loss of signal coherence? What are appropriate stochastic models for this region?
- What are the acoustic effects of surface waves and associated bubble plumes on the different classes of acoustic paths? What are the relative contributions of rough surface scattering versus bubble plume attenuation/refraction on phase and transmission loss variability?
- How are ambient sound fields modified by the oceanographic processes happening on rapid time scales? How does the rapid evolution of storms, both nearby and distant, affect wind generated ambient sound?
- How can acoustic data inform oceanographic measurements about the water masses present in the JMCh? Can the acoustic data be used to constrain data assimilating ocean circulation models?

4.1.3. Process Cruise Observations

The cruises in 2022 and 2023 to deploy and recover the moored array will also serve as process cruises, where specific oceanic features will be targeted and sampled. The process experiments may target some regions that have been well sampled historically, but without the focus on rapid changes of the upper ocean that are central to NORSE. For example, the ongoing observing systems maintained by Fer's group at the University of Bergen, Norway, provide invaluable information on the seasonal, mesoscale, and finescale evolution of the ocean along the Norwegian shelf break and Mohns Ridge, as well as in the Lofoten Basin eddy. They may also target areas that have not been studied extensively, including high-resolution surveys of the frontal dynamics near Jan Mayen.

Physical Oceanography

The physical processes that set the complex three-dimensional structure of sound speed in the upper ocean include sometimes strong surface forcing, frontal and other submesoscale instabilities that facilitate subduction, lateral stirring, and turbulent mixing. Many of those have timescales of hours or days, and their interplay during strong surface forcing events can drastically alter acoustic channels. A key feature of interest is the three-dimensionality of many of these processes. Some of the processes are fundamentally three-dimensional (subduction), but near regions of strong lateral density gradients even nominally one-dimensional processes (e.g., mixed layer deepening during strong wind events) can play out very differently on either side of a front, leading to resultant adjustments and secondary circulation.

Though shipboard sampling does not allow the large volume of statistics and long-term seasonal view of some of the autonomous assets, it provides complementary information in the form of high-resolution imaging of the relevant physical processes. A crucial component of successful sampling will be targeted combinations of shipboard profiling with short-term asset deployments. For example, rapid simultaneous profiles from a ship and the Drogued Buoy Air-Sea Interaction System (DBASIS) on either side of a front can reveal the similarities and differences to mixed layer evolution with different initial stratification, for the same surface forcing / storm event. Coordinated deployment of wave gliders, ocean gliders, and drifters provide invaluable contextual information on local vorticity, mesoscale strain and shear rates, turbulent dissipation, as well as water mass context. Similar combinations of tools have been used successfully in the recent NISKINe, SODA, and MISO-BoB experiments.

Acoustics: Mobile Sources and Receivers

Without the constraints of sampling within the moored array, the process cruises can focus on acoustic propagation across specific features, and characterize the acoustic and physical environment using a mobile network of sources and receivers. Sources will be deployed on the DBASIS, for example, with receiving arrays towed from gliders. The process cruises will use all resources available, including ship sampling, to characterize the ocean and collect the data necessary to predict its evolution.

Science Questions and Anticipated Outcomes

Measurements from the mobile assets will address questions about ocean processes, acoustic propagation, and ambient sound in the open ocean removed from the bathymetric effects of the Jan Mayen fracture zone.

- How do 1D forcing and 3D circulations conspire to set upper ocean sound speed processes, especially during strong surface forcing events? What are the dominant physical processes, and how well do we understand them?

- What are the effects of small to submesoscale to mesoscale fronts and eddies subjected to strong atmospheric forcing on acoustic propagation?
- What type of physical measurements capture the relevant physics accurately, or accurately enough, to allow for decent near-real time prediction of acoustic propagation pathways?
- Can the strong sound speed gradients associated with sloping isopycnals that define the fonts and eddies produce observable out-of-plane propagation effects?

4.2. Modeling Approach

Ocean modeling will be employed to support cruise planning and at-sea decision making. Additionally, process models will also be employed during the data analysis phase to address the rapid evolution of the surface ocean under strong forcing. These models will be realistic domain general circulation models along with idealized large eddy simulation (LES) models that can predict the turbulent evolution of the SBL. Specific objectives are to:

- Understand the processes that result in deep mixing events in response to resonant winds and surface waves

- Quantify the degree of coupling between atmospheric cyclone development or propagation and deep mixing events

- Identify the main turbulence production terms (e.g., shear production, turbulence transport, buoyancy production) that generate strong entrainment mixing at the SBL base and how they are related to surface forcing

- Examine how ocean mixing parameterizations perform under conditions with strong surface forcing

The modeling analysis and data will be coordinated with and shared with the observational efforts to address the project questions and anticipated outcomes.

Cooperation with ongoing Norwegian modeling efforts is already underway. Notably we have already obtained land surface model estimates of freshwater discharge from Jon Albretson at the Norwegian Institute of Marine Research. These data are essential for long-term simulations of frontal structures in the Nordic Seas.

General circulation modeling will include simulations using the Regional Ocean Modeling System (ROMS; *Shchepetkin and McWilliams*, 2005) ocean model (Fig. 7) and the Coupled Ocean–Atmosphere–Wave–Sediment Transport (COAWST) model (*Warner et al*., 2010). COAWST is a regional coupled ocean–atmosphere model based on the Weather Research and Forecasting (WRF; *Skamarock et al*., 2008) atmosphere model and the ROMS ocean model. Simulations with ROMS and COAWST will be used in a quasi-operational mode during the NORSE field campaigns to provide mesoscale context for process experiments. Numerical studies of the physics of rapid mixing will include simulations using the ocean LES model described in *Skyllingstad et al*. (1999), with typical computational domain sizes roughly 2 km in the horizontal and up to 500 m depth, depending on the specific mixing event. Fronts will be considered following the approach described in *Skyllingstad and Samelson* (2020).

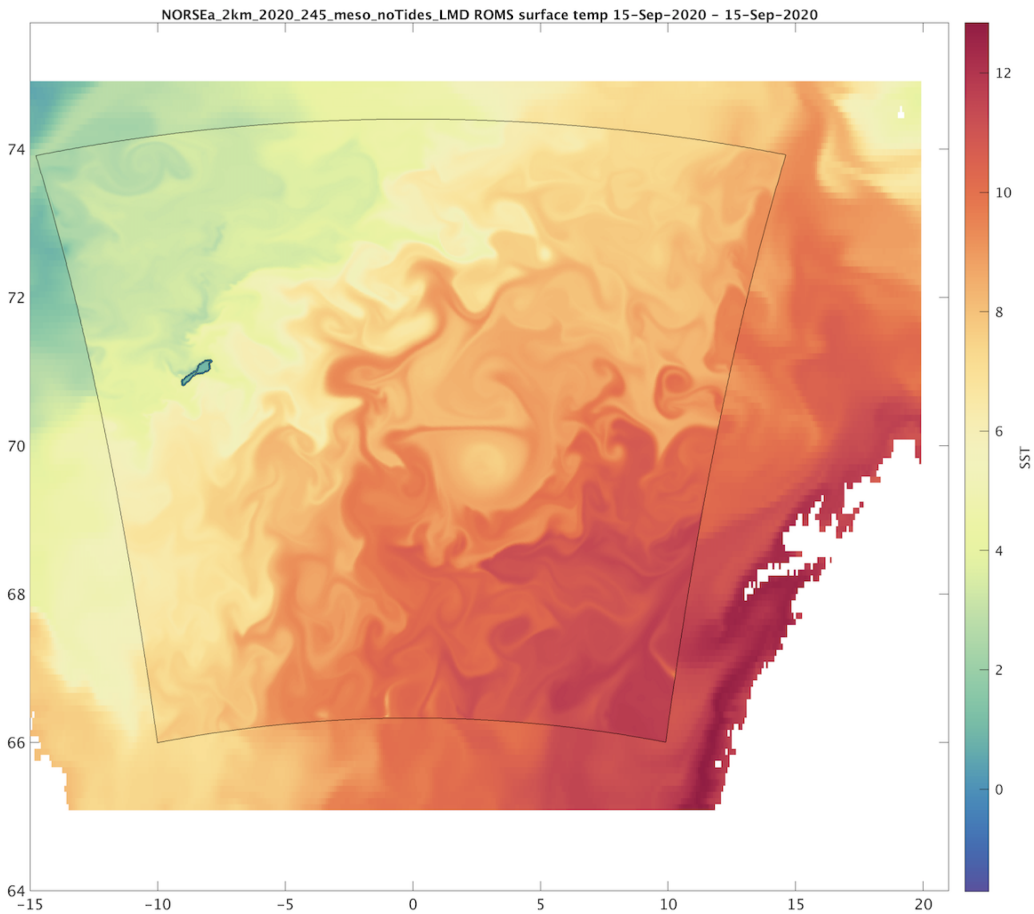

Figure 7. Example hindcast simulation of the Nordic Seas. The outer region is the GLORYS12V1 Mercator Ocean Model simulation GLOBAL_REANALYSIS_PHY_001_030 and the inset is a nested 2-km simulation using the ROMS ocean modeling system.

LES models will focus primarily on cases matched to events observed during the field program, with emphasis on rapid mixing forced by wind or wave action and strong surface heat flux, with forcing and initialization fields based on observed data supplemented by model analyses. The interaction between frontal and turbulent processes will be explored in connection with NORSE observations in areas with density fronts, where instabilities may arise from wind forced and geostrophic shear and from surface forced convection.

Regional models will be used to simulate energy transport by inertial gravity waves forced by surface winds and to study cases with strong cooling and widespread rapid mixing with convection and wind forcing. The observed evolution of the SBL in these cases will be compared with regional model and LES simulations to assess and understand the performance of the regional model turbulence parameterizations under conditions with severe surface forcing.

Acoustic propagation modeling will be conducted for physical fields based on NORSE field observations and the associated ocean physical modeling. The focus of the acoustic modeling will be on mid-frequency (wavelengths of 1–3 m) acoustic propagation and the effects of temporal and three-dimensional spatial variability in the upper ocean on acoustic pathways and transmission loss over ranges up to 100 km (e.g., Fig. 5). A variety of acoustic propagation models will be used, based on parabolic equations, ray tracing, wavenumber integration and fast-field methods, normal modes, and other standard approaches (*Jensen et al*., 2011). For parabolic equation solutions, see Figs. 1 and 6. The focus of this modeling will be to explore and assess the dependence of acoustic propagation and transmission loss on the rapidly varying near-surface physical fields, as well as to improve quantitative understanding of the requirements for characterization of those fields as is necessary for accurate prediction of sound propagation in the NORSE region.

4.3. Timing and Logistics

4.3.1. Pilot Cruise (R/V *Armstrong*), 1 September – 5 October 2021

The ship will support autonomous observations using an array of surface drifters, buoyancy driven gliders, a Wave Glider, and floats to make advances towards the general NORSE objectives to provide a better understanding of the coupled processes that drive rapid changes in the upper ocean at high latitudes, and improve predictive capability for sound propagation, transmission loss, and surface duct formation. The pilot cruise aims to collect data that will help planning of the main field experiments of 2022 and 2023.

4.3.2. Process Cruise and Mooring Array Deployment, Summer/Fall 2022

Goals of the intensive observation periods (IOP) during the 2022 cruise are mooring deployment, deployment and recovery of autonomous assets, and shipboard process sampling. Vessel requirements include i) space for a significant science party (20+) to encompass representation of acoustic teams, shipboard process teams, autonomous sampling teams, and international colleagues; ii) A-frame and winch capability for open ocean mooring deployment and recovery; iii) deck space for placement and operation of multiple shipboard profiling systems and winches; and iv) overall stability, so work may continue during strong surface forcing/storm conditions. Timing requirements are somewhat flexible, but the ideal time is late enough in the summer that some atmospheric storm events have begun to arrive (strong surface forcing), but conditions are not yet so severe as to limit shipboard work. September and October are ideal times; during these months the summer stratification gives way to autumn mixed layer deepening, allowing sampling of the changing physics and acoustic pathways throughout that process. Potential ports include Reykjavik, Bergen, and other ports further north along the Norwegian coast.

4.3.3. Charters in Late Winter/Early Spring 2023

Opportunities to deploy assets from Iceland and Norway are described here. The Marine and Freshwater Research Institute (MFRI) could charter some days during the winter and spring, with points close to NORSE that could be used (Fig. 8). The Bjerknes Centre for Climate Research at the University of Bergen has three ongoing glider missions with G3s (Fig. 9).

4.3.4. Mooring Array Recovery, Summer/Fall 2023

The mooring recovery cruise in 2023 will also serve as a process cruise and will likely be the core of another IOP. With the requirement that good weather is needed to recover the moorings, the cruise still needs to be scheduled (and a ship identified).

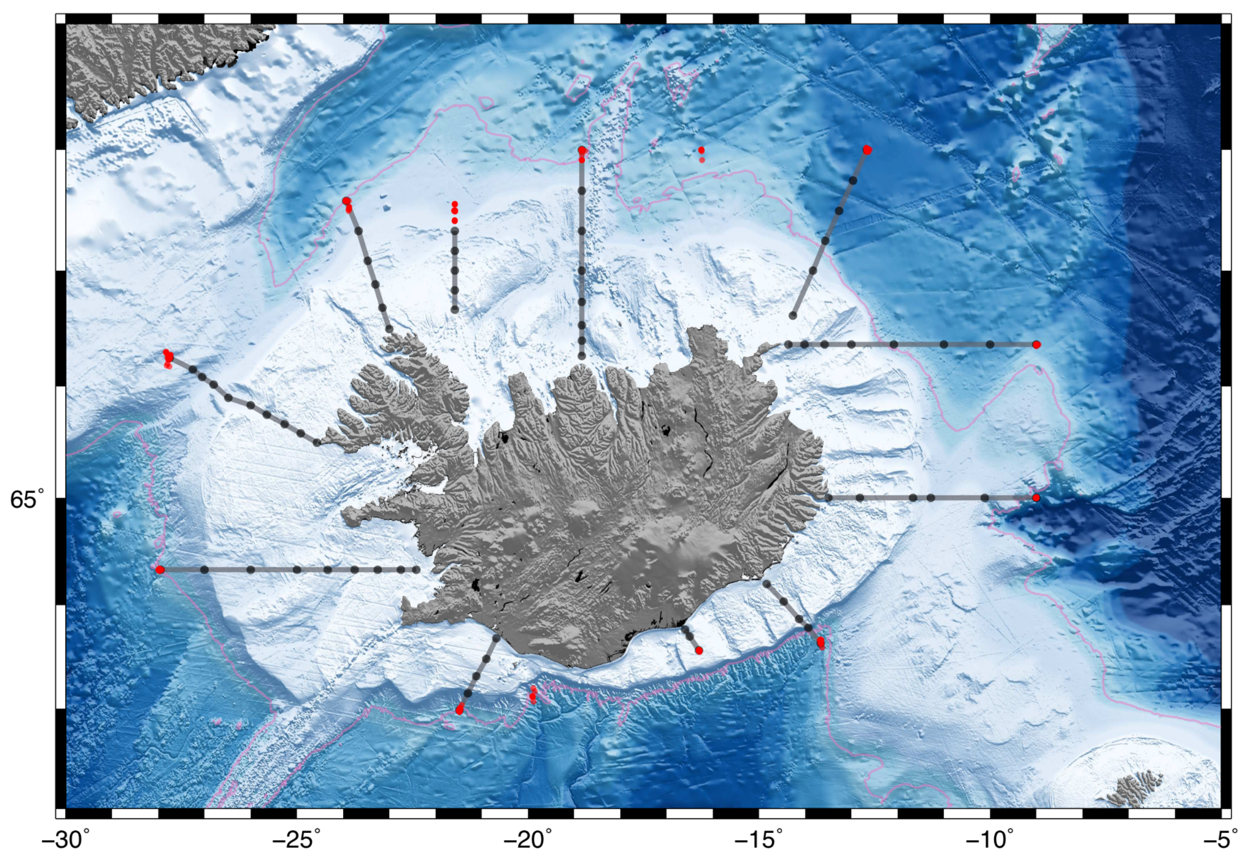

Figure 8. Typical hydrographic stations conducted by Hafro four times every year. The northeastern most stations could be suitable for NORSE asset recovery or deployment in 2023.

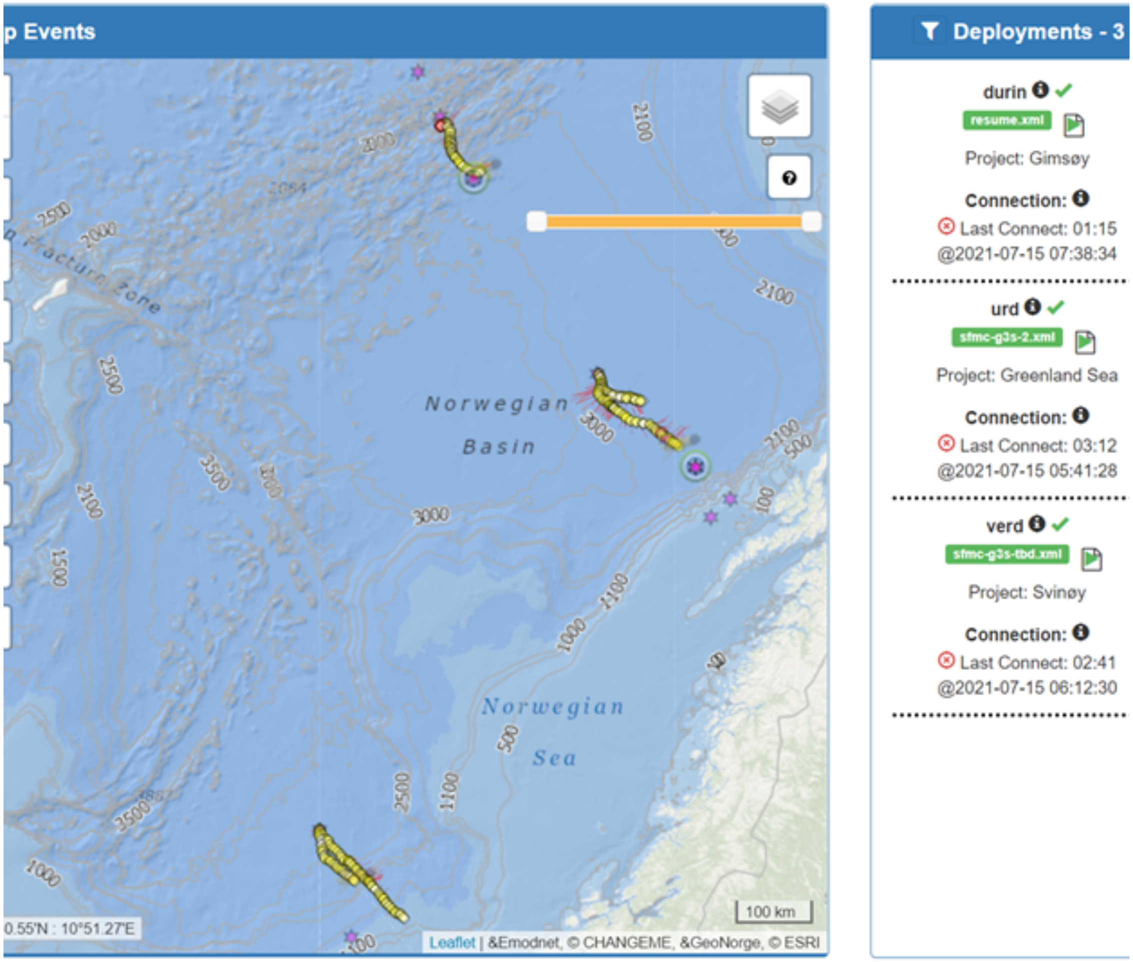

Figure 9. Locations of glider missions conducted three times each year by the Bjerknes Centre for Climate Research at the University of Bergen.

5. Resources and Program Components

5.1. Physical Oceanography

5.1.1. UUVs (Gliders)

Gliders fly using their buoyancy relative to the oceanic stratification and the aerodynamic lift generated by their body and wings. Typically, they achieve speeds of half-a-knot relative to the ambient environmental flow, and sample between the surface and 1000 m (or shallower) depth. Sampling includes measurements from a CTD, optical sensors, and ocean velocity structure as measured by Doppler current profiles. Three glider classes will be used for our 2022/2023 study: Seagliders operated by APL-UW (Rainville, Lee, and Johnson), Teledyne-Webb Slocum gliders operated by APL-UW and UAF (Shapiro and Simmons), and an ALSEAMAR SeaExplorer glider operated by VIMS (Gong and Ferris).

Seaglider and Seaglider Extended Range (4–6)

- Endurance: 6–8 months or up to 1 yr (with managed sampling); annual cycle coverage
- Profiles: 0–1000 m, 4–6/day
- Sensing: CTD, turbulence microstructure (temp and shear; optional), ADCP, passive acoustics (~1–80 kHz)

Slocum Glider (~2)

- Endurance: 4–6 months; annual cycle coverage possible
- Profiles: 0–1000 m, 4–6/day
- Sensing: CTD, turbulence microstructure (temp and shear; optional), towed hydrophone array (short missions)

SeaExplorer X2 (1)

- Endurance: 1 month (ADCP + microrider) with rechargeable battery
- Profiles: 0–500 m, 10–12/day. Will adapt dive profiles to capture features of interest (flow–topography interaction, fronts) based on real time analysis. Horizontal resolution is 470 or 940 m (if sampling only downcast or upcast) when diving 500 or 1000 m.
- Missions: 2–4 total. Deployment (recovery) at the beginning (end) of each process cruise, with possible recharge and redeployment at the end of each process cruise and opportunistic recovery via the November/December annual Hafro cruise run by the Icelandic Marine and Freshwater Research Institute (MFRI).
- Sensing: RBR Legato CTD, EcoPUCK, dissolved oxygen, Nortek AD2CP, Rockland Microrider

Photo courtesy of U. Tokyo

Slocum Glider (5)

- Operated by Fer, Våge, Brakstad, and Elliott (University of Bergen)
- Endurance: 4–6 months; annual cycle coverage possible
- Profiles: 0–1000 m, 4–6 profiles/day; possibly occupy lines defined by other programs
- Sensing: CTD, one glider with turbulence microstructure (short missions)

5.1.2. USV Sensing (Surface)

Wave Glider (SV3)

- Operated by Merrifield (SIO)
- Endurance: 4–6 months; contributor to annual cycle coverage
- Sensing: CTD, ADCP, waves, atmosphere

Wave Glider (SV3)

- Operated by Thomson and Zeiden (APL-UW)
- Endurance: 4–6 months; contributor to annual cycle coverage
- Sensing: CTD, ADCP, waves, atmosphere (including direct flux wind stress), profiling CTD winch (8–150 m)

5.1.3. Lagrangian Sensing

- Operated by Centurioni (SIO) and Poulain (CMRE)
- Deployments: Surface, multi-month, not recovered

Surface Velocity Program Drifter

SVPs are drogued at 15 m depth, equipped with sea surface temperature (SST) sensors, and will be deployed in coherent mesoscale and submesoscale arrays to measure the vorticity of the background circulation.

Lagrangian surface drifters equipped with a barometer (SVP-B) are known to have a sizeable beneficial effect on atmospheric reanalysis products as well a Numerical Weather Prediction (NWP) models. Atmospheric pressure measurements from drifters are an essential component to constrain the large-scale sea level air pressure field accurately, and to correct errors of numerical atmospheric models in case of fast evolving storms and explosive cyclogenesis (*Centurioni et al*., 2017a; *Centurioni*, 2018; *Horányi et al*., 2016). The SVP-B drifter is drogued at 15 m depth and will therefore measure ocean currents while sensing the atmospheric pressure at the same time. The objective of deploying an array of SVP-B drifters is to support real time numerical weather prediction and the computation of reanalysis wind and pressure fields, such as ERA-INTERIM from the European Centre for Medium-Range Weather Forecasts (ECMWF).

Three SVP drifters, equipped with hydrophones (narrow and wide bands), and two profiling floats, equipped with a SBE CTD and compact volumetric acoustic sensor, are still prototypes so we plan to deploy and recover them intermittently during the cruise. Some reduced acoustic data will be telemetered via satellites, but most of the data should be downloaded after the recovery of the instruments. These instruments have to be 'mostly recovered'.

Minimet Drifter

The MiniMet drifter, a variant of the SVP-B drifter, has been used successfully in several ONR and NOAA experiments to measure the surface sea level pressure and the surface horizontal wind (*D'Asaro et al*., 2013; *Hormann et al*., 2014; *Zedler et al*., 2009). The modern MiniMet drifter uses a high-quality sonic anemometer and an internal compass to measure the wind velocity. Like the SVP-B drifter, the MiniMet is drogued at 15 m depth to measure ocean currents. Both the Minimet and the SVP-B drifters can be air deployed. In situ wind observations will be valuable to validate wind reanalysis products.

Directional Wave Spectra Drifter

Directional Wave Spectra Drifters (*Centurioni et al*., 2017b) use GPS technology to measure the directional spectra of surface gravity waves across the frequency range 0.03–0.50 Hz, which is characteristic of swell and wind waves. Because the DWSD are undrogued, they will not be used to measure ocean currents.

Floats (ALAMO and ALTO)

- Operated by Jayne (WHOI)
- Endurance: Multi-month missions, not recovered or partly recovered

During the NORSE pilot program in 2021, we plan to deploy and operate 2–3 ALAMO profiling floats. The floats will collect profiles of upper ocean temperature and salinity. The float communicates via Iridium and uses GPS for position sensing. Expected endurance is a few months, but we hope to recover the float at the end of the cruise.

Drogued Buoy Air–Sea Interaction System

- Operated by Farrar (WHOI) and Lucas (SIO)
- Deployments: Two full-scale systems (on process cruises only), and two 'expeditionary' systems that may not be recovered

Under previous ONR funding, a SIO/WHOI collaboration led to the successful integration of a WHOI air-sea flux buoy with a SIO Wirewalker vertical profiling vehicle. DBASIS buoys were deployed in the Bay of Bengal in 2018 (1) and 2019 (3), where they measured the bulk air–sea fluxes and the response of the ocean boundary layer simultaneously in real time and in high resolution. The drogued drifting design allowed for a process study deployment at much lower cost than that of several deepwater moorings. Cost savings were also achieved in design changes to the surface buoy, and by the reduction in subsurface instrumentation facilitated by the vertical profiling vehicle. The deployments indicated our capacity to field such systems, and demonstrated their ability to resolve the processes at work in the open ocean during strong monsoon forcing in the context of very shallow ocean mixed layers.

Measurements gathered by a 1-MHz profiling ADCP mounted on the Wirewalker showed the ocean's complicated shear response to strong atmospheric forcing, with frequency resolution of many cycles per hour and vertical resolution of < 2 m through the upper ocean and ocean mixed layer. Optical data indicated strong changes in attenuation over the course of the deployment due to both biological processes and the entrainment and export of sediment-laden coastal water by the mesoscale eddy field. These data are crucial to test assumptions in the 1D and submesoscale parameterizations used in operational forecast models. The property evolution that arises because of the sheared ocean response to wind forcing directly impacts mid-frequency transmission loss.

The essential elements of the DBASIS system are: (1) a WHOI surface buoy carrying high-quality surface meteorological instruments, a data logger, and satellite (Iridium) transmitters, (2) a Scripps Wirewalker profiling instrument package to measure temperature, salinity, velocity, and bio-optical properties at high vertical resolution, (3) fixed-depth subsurface instruments for temperature, salinity, and velocity, and (4) several 'X-wing' drag elements deployed at around 200 m depth.

SWIFTs

- Operated by Thomson and Zeiden (APL-UW)
- Deployments: 6 systems on cruises only with plans to recover all surface drifters

SWIFT drifters measure turbulence at the ocean surface in a wave-following reference frame (*Thomson*, 2012). The turbulence measurements use up-looking pulse-coherent Doppler profilers (2 MHz). Secondary measurements include directional wave spectra, surface winds, salinity, water temperature, air temperature, and surface images. Capabilities include onboard processing, Iridium SBD data telemetry, AIS tracking, and month-long endurance. A passive hydrophone

(Loggerhead SNAP) can be suspended from the drifter at 10 m to record ambient sound from breaking surface waves and rain.

5.1.4. Ship-Based Sensing

FastCTD and PADS

The original SIO FastCTD system (Savage and colleagues) has been upgraded to accommodate a microstructure sampling capability, to include optical channels (WETLabs ECOPuck with Chlorophyll *a*, CDOM, and 532 nm backscatter), and to run on a direct-drive winch built on a frameless motor platform. The FastCTD system will be used to obtain very rapid profiles of temperature and salinity while steaming at 2–5 knots. The winch is typically mounted in the port quarter, with the control station just forward and inboard. The boom, 32' long, rests directly forward when the system is not in use. The FastCTD "fish" is overboarded by swinging the boom outboard manually with taglines. It can cycle either the FastCTD fish (5–6 m/s descent rate, 4 m/s ascent rate; equipped with SBE-49 and WETLabs ECOPuck) or a microstructure instrument (0.7–1 m/s descent rate, 3 m/s ascent rate; MOD Epsi with a SBE 49).

During this cruise the FastCTD can regularly switch back and forth between deployment modalities. With the very low drag FastCTD fish and the direct-drive winch and sheave systems, profiling speeds are fast (> 5 m/s), and can be profiled at ship speeds of up to 5 knots. With the purposefully high drag (to resolve the cm scales of turbulent shear) microstructure profiler, ship speeds were typically limited to 2 or 2.5 knots. Deep profiles are possible (~1000 m), but the primary science questions of interest to NORSE will necessitate shallower profiling depths with fast repeat time (minutes).

A new Phased Array Doppler System (PADS) is in development with DURIP funds. PADS images an angular sector of ocean currents at any one time, giving true snapshots of coherent structure. The new system is towed from a similar style winch as the FastCTD, with a 'smart' tensioning system that allows for level flight even from a heaving ship. This system is being designed to fly outboard, from the opposite quarter as the FastCTD, with the idea that they will be deployed together. While the FastCTD (or microstructure swap-out) gives vertical profiles, the towed PADS will simultaneously give a swath view of detailed structures of mixed layer and sub-surface frontal instabilities, allowing better dynamical interpretation. Deployment of both the FastCTD and towed PADS will require two substantial winches on deck.

Bow Chain and uCTD

During the pilot cruise, an underway CTD (uCTD) system can be mounted on the fantail of the ship such that it does not interfere with other operations. On a moment's notice, a cast can be obtained when there is an opportunity. A single cast to 200 m, recording temperature, pressure, and salinity, only takes about 5 min. The system can also be used in tow-yo mode at a variety of ship speeds (0–12 kts) and during transits. Two operators from the science party need to be on deck at all times during operations (with communication to the bridge).

A bow chain system will be mounted on the ship to measure finescale structure at fronts. The system can only be deployed when the ship is going 4 knots or less, and when the sea state is not too rough, otherwise the sensors collide destructively with the side of the ship. The 'bow commander' winch will be installed in port and allows the sensor chain to be deployed quickly, in ~15 min. We anticipate deploying it for 8–12 hr intermittently to sample an interesting front while using the uCTD to get the deeper structure more sparsely. An electric winch is used to lower the 200 lb weight. The sensors themselves are attached to a clip-in-clip-out separate line, which is tied off on a capstan near the bow and becomes load bearing underway.

5.2. Ocean Acoustics

5.2.1. Moored Array

The PErsistent aCoustic Observation System (PECOS), operated by Ballard and Sagers (ARL/UT), is an autonomous recording system capable of yearlong recording at sample rate of 8192 Hz with a 10% duty cycle. PECOS has an atomic clock time base, redundant recording systems, and very low self-noise. A new array is being fabricated for NORSE. The array will have 52 hydrophones (HTI-90), and it can be configured as a vertical, horizontal, or L-shaped array. The minimum spacing between hydrophones is approximately 1 m. The PECOS instrument pressure vessels are depth rated for 500 m, and the mooring sled is configured for a seafloor deployment.

A moored acoustic source will be deployed for NORSE. The source will broadcast 500 Hz to at least 1 kHz at a level of 170 dB re 1 μPa. The source will be programmable with a yearlong endurance and atomic clock time base for synchronization with PECOS. The source will have a nominal broadcast schedule of 135-s-long transmissions every four hours. The source projector is rated to a depth of 300 m, and the mooring will be designed for deployment in the ocean basin.

Depending on the deployment location, propagation distances of 30–50 km are being considered. The length of the propagation path will depend on source level, array gain, and ambient sound level.

5.2.2. Mobile Sources

Limited duration shipboard acoustic source operations are planned using a U.S. Navy J-9 or J-13 acoustic projector. These sources have been operated routinely by OASIS personnel from UNOLS vessels, and specifications can be furnished upon request. The J-9 is lightweight (20 lbs) and easily hand-deployed over the side of the support vessel to depths of approximately 50'. The J-13 is heavier, approximately 150 lbs, and deployed with a bottle of compressed air to support pressure compensation at depth. It can be deployed to a depth of 300'. The J-13 requires the use of a hydraulic winch and davit to deploy, and is typically deployed for 2–4 hr of continuous acoustic transmission. A deployment or recovery cycle can be expected to take 10–15 min with the assistance of experienced ship's crew. Source operations will generally be requested daily for limited periods of time to transmit acoustic signals designed to support evaluation of hydrophone array straightness and in situ measurement of transmission loss. Daily measurements of sound speed stratification using CTD, and current profiles using ship's ADCP, will also be required to support array performance characterization.

Drifting Sources

- Operated by Duda and Farrar et al. (WHOI)
- Configuration: On deep-drogued flux systems
- Sources: 550 kHz or 750 kHz (both 200+ Hz BW), which can be modified to transmit in a different band
- Receivers: Develogic (4-phones) and modestly priced Sound Trap receivers

5.2.3. Receiving Arrays and Hydrophones

OASIS (Abbot) plans to deploy a Slocum G2 (Shapiro, APL-UW) instrumented with a towed receiving array to collect data on the spatial and temporal variability of the acoustic sound distribution concurrently with oceanographic data to support a detailed examination of the link between oceanographic variability and acoustic environment characteristics. The intention will be to deploy the Slocum G2 in areas that are being concurrently sampled with oceanographic instrumentation deployed by the rest of the NORSE science team. Ideally, concurrent oceanographic data on temperature and density stratification, current profiles, sea state, wind speed and direction, will be required to support the physical interpretation of measured acoustic results. Ideally, the glider mission length we are seeking is on the order of 10–15 days, with multiple missions, if possible. Initially, there may be a few shorter deployment cycles for engineering shakedown and system validation. We are planning to exfiltrate some limited acoustic noise data and array health status messages via Iridium during each glider surfacing. The only way to download and back up array element data will be to recover the glider and make a hardwire connection in the lab.

5.2.4. Ambient Sound (Including Transmissions) Passive Acoustics

- On many surface drifters for multi-month duration
- On some Seagliders/SGX for multi-month duration
- On some SWIFTs during process cruises
- On deep-drogued flux systems during process cruises

6. Data Dissemination

The NORSE program will employ a lightweight data distribution structure consisting of a password protected, central repository for storing and distributing project data and model output, along with associated documentation. To promote broad use of the data, and to encourage active collaboration, open access, governed by the NORSE program data policy (Section 7), will be provided to all NORSE investigators.

To facilitate use in numerical efforts, to provide guidance for ship-based efforts, float deployments, and mobile platforms, and to assist collaborating programs, data will be posted as rapidly as possible. Each observational component will plan for a hierarchy of data release that should include:

1. Quick-release products that incorporate minimal quality control and processing.
2. Delayed-mode products, delivered in time for use in the analysis phase, that incorporate full quality control, processing, and correction. These products will be versioned to accommodate updates as additional issues are identified and corrected.

Delayed-mode data should be accompanied by full documentation describing platform, instrument, sensors (including precision and accuracy), quality control, calibration, and correction procedures.

A Data Coordination Working Group will be formed from the NORSE PIs. This team will be responsible for working with the various program components to establish mutually agreed upon data formats and to coordinate delivery, distribution, and archiving of observational data and model output.

7. Data Policy

The ONR Northern Ocean Rapid Surface Evolution (NORSE) program consists of all investigators participating in the integrated efforts associated with the NORSE Departmental Research Initiative (DRI). This includes the core team of ONR-supported investigators funded directly by the NORSE DRI and investigators funded though other mechanisms, but coordinated as part of the NORSE program. NORSE DRI data will include observations from field programs, remote sensing data, and model results, all of which will be treated equally for the purposes of the program data policy. All data are collected for basic research and will be unclassified.

Given the complex nature of the science questions and challenges associated with collecting the necessary observations, the success of the NORSE program depends on open, effective data sharing and collaboration. To facilitate sharing of data and collaboration between NORSE scientists, the NORSE DRI will establish a program data archive. To further promote and support sharing and collaboration, the NORSE DRI specifies policies to govern the use of data collected under the program.

7.1. Data Use

It is not ethical to publish data without proper attribution or co-authorship. The data are the intellectual property of the collecting investigator(s). Similar standards apply to theoretical ideas, code, and analysis techniques newly developed for the NORSE program.

The intellectual investment and time committed to the collection of a data set entitles the investigator to the fundamental benefits of the data set. Publication of descriptive or interpretive results derived immediately and directly from the data is the privilege and responsibility of the investigators who collect the data.

There are two possible actions for any person making substantial use of NORSE data sets, both of which require discussion with and permission from the data collector:

1. *Expectation of co-authorship*
   This is the usual condition. Scientists making use of the data should anticipate that the data collectors would be active participants and require co-authorship of published results.

2. *Citation and acknowledgment*
   In cases where the data collector acknowledges the importance of the application but expects to make no time investment or intellectual contribution to the published work, the data collector may agree to provide the data to another scientist provided data reports are properly cited and the contribution is recognized in the text and acknowledgments.

Authors must share and discuss manuscripts with all NORSE investigators who contributed data prior to submission anywhere.

Agreements about publication, authorship, or citation should be documented at a minimum by email between the investigators.

7.2. Roles and Responsibilities

Principal investigators who are responsible for the collection of observational data or generation of model data during the NORSE DRI are considered participating NORSE DRI scientists and may request data from and provide data to other participating scientists. Participating scientists have primary responsibility to quality control their own data and make it available to the rest of the NORSE participating scientists on a timely basis.

Data should be released as soon as possible, through the NORSE data archive, along with documentation that can be used by other researchers to judge data quality and potential usefulness.

The data contained in the archive are made available even though they may not be "final" (i.e., error free) data so it is the responsibility of the user to verify the status of the data and to be aware of its potential limitations.

Participating scientists who wish to use others' data sets are responsible for notifying those principal investigators of their intent and inviting collaboration and/or co-authorship of published results.

Participating scientists must consider the interests of graduate students and postdocs before publishing data. Plans for graduate student and postdoc projects must be discussed openly and effort made by all NORSE DRI investigators to facilitate and protect these efforts.

For the duration of the NORSE DRI (2021–2024), program data will be restricted to NORSE DRI investigators. Dissemination beyond program investigators will require the agreement of NORSE DRI investigators and the cognizant ONR program managers. After this time, NORSE DRI participating investigators are required to submit their data to the official data management facility, which will be determined during the DRI.

The NORSE DRI prohibits third party data dissemination; participants are not allowed to redistribute data taken by other NORSE investigators.

All potential users who access the data will be reminded of the NORSE DRI commitment to the principle that data are the intellectual property of the collecting scientists.

Program sponsors of participating scientists may arbitrate and reach agreement on data sharing questions when they arise.

8. References

Ainslie, M.A. (2005). Effect of wind-generated bubbles on fixed range acoustic attenuation in shallow water at 1-4 kHz. *J. Acoust. Soc. Am*., 118, 3513, doi:10.1121/1.2114527.

Asselin, O., L.N. Thomas, W.R. Young, and L. Rainville (2020). Refraction and straining of near-inertial waves by barotropic eddies. *J. Phys. Oceanogr*., 50, 3439-3454, doi:10.1175/JPO-D-20-0109.1.

Ballard, M.S., B.M. Goldsberry, and M.J. Isakson (2015). Examining three-dimensional propagation over a cosine shaped hill using normal modes. *J. Comput. Acoust*., 23, doi: 10.1142/S0218396X15500058

Beilis, A., and F.D. Tappert (1979). Coupled mode analysis of multiple rough surface scattering. *J. Acoust. Soc. Am*., 66, 811-826, doi:10.1121/1.383685.

Bodner, A.S., B. Fox-Kemper, L.P. Van Roekel, J.C. McWilliams, and P.P. Sullivan (2019). A perturbation approach to understanding the effects of turbulence on frontogenesis. *J. Fluid Mech*., 883.

Bosse, A., and I. Fer (2019a). Seaglider missions in the Norwegian Sea during the PROVOLO project. Norwegian Marine Science Data Centre, https://doi.org/10.21335/NMDC-980686647.

Bosse, A., and I. Fer (2019b). Mean structure and seasonality of the Norwegian Atlantic Front Current along the Mohn Ridge from repeated glider transects. *Geophys. Res. Lett*., 46, 13,170–13,179.

Bosse, A., I. Fer, H. Søiland, and T. Rossby (2018). Atlantic water transformation along its poleward pathway across the Nordic Seas. *J. Geophys. Res. Oceans*, 123, 6428-6448.

Bosse, A., I. Fer, J.M. Lilly, and H. Søiland (2019). Dynamical controls on the longevity of a non-linear vortex: The case of the Lofoten Basin eddy. *Sci. Rep*., 9, 13448, doi:10.1038/s41598-019-49599-8

Callies, J., R. Ferrari, J.M. Klymak, and J. Gula (2015). Seasonality in submesoscale turbulence. *Nat. Comm*., 6, doi: 10.1038/ncomms7862.

Centurioni, L., et al. (2017a). Northern Arabian Sea Circulation–Autonomous Research (NASCar): A research initiative based on autonomous sensors. *Oceanography*, 30, 74-87.

Centurioni, L.A. Horányi, C. Cardinali, E. Charpentier, and R. Lumpkin (2017b). A global ocean observing system for measuring sea level atmospheric pressure: Effects and impacts on numerical weather prediction. *Bull. Am. Meteorolog. Soc*., 98, 231-238.

Centurioni, L.R. (2018). Drifter technology and impacts for sea surface temperature, sea-level pressure, and ocean circulation studies. *Observing the Oceans in Real Time* (Springer International Publishing), pp. 37-57.

Cole, S.T., D.L. Rudnick, and J.A. Colosi (2010). Seasonal evolution of upper-ocean horizontal structure and the remnant mixed layer. *J. Geophys. Res. Oceans*, 115, doi: 10.1029/2009JC005654.

Colosi J., and D. Rudnick (2020). Observations of upper ocean sound-speed structures in the North Pacific and their effects on long-range acoustic propagation at low and mid-frequencies. *J. Acoust. Soc. Am*., 148, doi.org/10.1121/10.0002174.

Damerell, G.M., K.J. Heywood, D. Calvert, A.L. Grant, M.J. Bell, and S.E. Belcher (2020). A comparison of five surface mixed layer models with a year of observations in the North Atlantic. *Prog. Oceanogr.*, *187*, 102316.

D'Asaro, E.A., P.G. Black, L.R. Centurioni, Y.-T. Chang, S.S. Chen, R.C. Foster, H.C. Graber, P. Harr, V. Hormann, R.-C. Lien, I.-I. Lin, T.B. Sanford, T.-Y. Tang, and C.-C. Wu (2013). Impacts of typhoons on the ocean in the Pacific. *Bull. Am. Meteorolog. Soc*., 95, 1405-1418.

du Plessis, M., S. Swart, I.J. Ansorge, A. Mahadevan, and A.F. Thompson (2019). Southern Ocean seasonal restratification delayed by submesoscale wind–front interactions. *J. Phys. Oceanogr*, 49, 1035-1053.

Dushaw, B.D., H. Sagen, and A. Beszczynska-Möller (2016). On the effects of small-scale variability on acoustic propagation in Fram Strait: The tomography forward problem. *J. Acoust. Soc. Am*., 140, 1286-1299.

Dzieciuch, M., W. Munk, and D.L. Rudnick, (2004). Propagation of sound through a spicy ocean, the SOFAR overture. *J. Acoust. Soc. Am*., 116, 1447-1462.

Fox-Kemper, B., R. Ferrari, and R. Hallberg (2008). Parameterization of mixed layer eddies. Part I: Theory and diagnosis. *J. Phys. Oceanogr.*, 38, 1145-1165.

Horányi, A., C. Cardinali, and L. Centurioni (2017). The global numerical weather prediction impact of mean-sea-level pressure observations from drifting buoys. *Q. J. R. Meteorolog. Soc.*, 143, 974-985.

Hormann, V., L.R. Centurioni, L.R. Rainville, C.M. Lee, and L.J. Braasch (2014). Response of upper ocean currents to Typhoon Fanapi. *Geophys. Res. Lett*., 41, 3995-4003.

Hosegood, P., M.C. Gregg, and M.H. Alford (2006). Sub-mesoscale lateral density structure in the oceanic surface mixed layer. *Geophys. Res. Lett.*, 33, doi:10.1029/2006GL026797.

Jensen, F.B., W.K. Kuperman, M.B. Porter, and H. Schimdt (2011). *Computational Ocean Acoustics* (Springer) 794 pp.

Johnson, L., C.M. Lee, E.A. D'Asaro, J.O. Wenegrat, and L.N. Thomas (2020). Restratification at a California current upwelling front. Part II: Dynamics. *J. Phys. Oceanogr.*, 50, 1473-1487.

Köhl, A. (2010). Variable source regions of Denmark Strait and Faroe Bank Channel overflow waters. *Tellus A*, 62, 551-568, doi:10.1111/j.1600-0870.2009.00454.x

Lin, Y.-T. (2019). Three-dimensional boundary fitted parabolic-equation model of underwater sound propagation, *J. Acoust. Soc. Am.*, 146, 2058-2067, doi:10.1121/1.5126011.

Messias, M.J., A.J. Watson, T. Johannessen, K.I.C. Oliver, K.A. Olsson, E. Fogelqvist, and J.R. Ledwell (2008). The Greenland Sea tracer experiment 1996–2002: horizontal mixing and transport of Greenland Sea intermediate water. *Prog. Oceanogr.*, 78, 85-105.

McWilliams, J.C., J. Gula, M.J. Molemaker, L. Renault, and A.F. Shchepetkin (2015). Filament frontogenesis by boundary layer turbulence. *J. Phys. Oceanogr.*, 45, 1988-2005.

Østerhus, S., T. Gammelsrød (1999). The abyss of the Nordic Seas is warming. *J. Clim.*, 12, 3297-3304.

Pham, H. T., and S. Sarkar (2018). Ageostrophic secondary circulation at a submesoscale front and the formation of gravity currents. *J. Phys. Oceanogr.*, 48, 2507-2529.

Phillips, O.M. (1985). Spectral and statistical properties of the equilibrium range in wind-generated gravity waves, *J. Fluid Mech.*, 156, 495–531.

Pollard, R.T., and R.C. Millard, Jr. (1970). Comparison between observed and simulated wind-generated oscillations. *Deep-Sea Res.*, 17, 813-821.

Price, J., R. Weller, and R. Pinkel (1986). Diurnal cycling: observations and models of upper ocean response to diurnal heating, cooling and wind mixing. *J. Geophys. Res.*, 91, 8411–8427.

Raghukumar, K., and J.A. Colosi (2014). High frequency normal mode statistics in a shallow water waveguide: The effect of random linear internal waves. *J. Acoust. Soc. Am.*, 136, doi:10.1121/1.4881926.

Raj, R.P., J.A. Johannessen, T. Eldevik, J. Ø. Nilsen, and I. Halo (2016). Quantifying mesoscale eddies in the Lofoten Basin. *J. Geophys. Res. Oceans*, 121, 4503-4521.

Raj, R.P., I. Halo, S. Chatterjee, T. Belonenko, M. Bakhoday-Paskyabi, I. Bashmachnikov, A. Fedorov, and J. Xie (2020). Interaction between mesoscale eddies and the gyre circulation in the Lofoten Basin. *J. Geophys. Res. Oceans*, 125, doi:10.1029/2020JC016102.

Rosenberg, A.P. (1999). A new rough surface parabolic equation program for computing low-frequency acoustic forward scattering from the ocean surface. *J. Acoust. Soc. Am*.,105, 144-153, doi:10.1121/1.424626.

Rudnick, D.L. (2004). Spice, internal waves, and sound speed in the upper ocean. *J. Acoust. Soc. Am*., 116, 2634-2634.

Sælen, O.H. (1990). On the exchange of bottom water between the Greenland and Norwegian seas. *Acta Geophys*., 3, 133–144.

Sanchez-Rios, A., R.K. Shearman, J. Klymak, E. D'Asaro, and C. Lee (2020). Observations of cross-frontal exchange associated with submesoscale features along the North Wall of the Gulf Stream. *Deep Sea Res. I*, 163, doi:10.1016/j.dsr.2020.103342.

Shao, Q., J. Zhao, K.F. Drinkwater, X. Wang, and Y. Cao (2019). Internal overflow in the Nordic Seas and the cold reservoir in the northern Norwegian Basin. *Deep Sea Res. I*, 148, 67-79.

Shchepetkin, A.F., and J.C. McWilliams (2005). The regional oceanic modeling system (ROMS): a split-explicit, free-surface, topography-following-coordinate oceanic model. *Ocean Mod.*, 9, 347-404.

Skamarock, W.C., J.B. Klemp, J. Dudhia, D.O. Gill, D.M. Barker, M.G. Duda, X.-Y. Huang, W. Wang, and J.G. Powers (2008). *A Description of the Advanced Research WRF Version 3*. NCAR Tech. Note NCAR/ TN-4751STR, 113 pp., doi:10.5065/D68S4MVH.

Skyllingstad, E.D., J. Duncombe, and R.M. Samelson (2017). Baroclinic frontal instabilities and turbulent mixing in the surface boundary layer, Part II: Forced simulations. *J. Phys. Oceanogr*., 47, 2429-2454.

Skyllingstad, E.D., and R.M. Samelson (2012). Baroclinic frontal instabilities and turbulent mixing in the surface boundary layer, Part 1: Unforced simulations. *J. Phys. Oceanogr*., 42, 1701-1716.

Skyllingstad, E.D., and R.M Samelson (2020). Instablility processes in simulated finite-width ocean fronts, *J. Phys. Oceanogr*., 50, 2781-2796, doi:10.1175/JPO-D-20-0030.1.

Skyllingstad, E.D., W.D. Smyth, J.N. Moum, and H. Wijesekera (1999). Upper ocean turbulence during a westerly wind burst: A comparison of large-eddy simulation results and microstructure measurements. *J. Phys. Oceanogr*., 29, 5-28.

Spall, M.A. (1995). Frontogenesis, subduction, and cross-front exchange at upper ocean fronts. *J. Geophys. Res. Oceans*, 100, 2543-2557.

Spall, M., M. Almansi, J. Huang T.W. Haine and R.S. Pickart (2021). Lateral redistribution of heat and salt in the Nordic Seas. *Prog. Oceanogr*., 196, doi:10.1016/j.pocean.2021.102609.

Spiro Jaeger, G., J.A. MacKinnon, A.J. Lucas, E. Shroyer, J. Nash, A. Tandon, and A. Mahadevan (2020). How spice is stirred in the Bay of Bengal. *J. Phys. Oceanogr*., 50, 2669-2688.

Suzuki, N., B. Fox-Kemper, P.E. Hamlington, and L.P. Van Roekel (2016). Surface waves affect frontogenesis. *J. Geophys. Res. Oceans*, 121, 3597-3624.

Swart, S., M.D. du Plessis, A.F. Thompson, L.C. iddle, I. Giddy, T. Linders, and S.A. Nicholson (2020). Submesoscale fronts in the Antarctic marginal ice zone and their response to wind forcing. *Geophys. Res. Lett*., 47, doi: 10.1029/2019GL086649.

Swift, J.H., and K.P. Koltermann (1988). The origin of Norwegian Sea deep water. *J. Geophys. Res*., 93, 3563– 3569, doi:10.1029/JC093iC04p03563.

Tandon, A., and C. Garrett (1994). Mixed layer restratification due to a horizontal density gradient. *J. Phys. Oceanogr.*, 24, 1419-1424.

Thomas, L.N. (2008). Formation of intrathermocline eddies at ocean fronts by wind-driven destruction of potential vorticity. *Dyn. Atmos. Oceans*, 45, 252-273.

Thomas, L.N., J.R. Taylor, R. Ferrari, and T.M. Joyce (2013). Symmetric instability in the Gulf Stream. *Deep Sea Res. II*, 91, 96-110.

Thomas, L.N., L. Rainville, O. Asselin, W.R. Young, J. Girton, C.B. Whalen, L. Centurioni, and V. Hormann (2020). Direct observations of near-inertial wave-refraction in a dipole vortex. *Geophys Res. Lett*., 47, doi:10.1029/2020GL090375.

Thomson, J. (2012). Wave breaking dissipation observed by SWIFT drifters. *J. Atmos. Ocean. Technol*., 29, 1866-1882.

Thomson, J., E. D'Asaro, M. Cronin, E. Rogers, R. Harcourt, and A. Shcherbina (2013). Waves and the equilibrium range at Ocean Weather Station P, *J. Geophys. Res*., 118, doi: 10.1002/2013JC008837.

Thompson, A.F., A. Lazar, C. Buckingham, A.C.N. Garabato, G.M. Damerell, and K.J. Heywood (2016). Open-ocean submesoscale motions: A full seasonal cycle of mixed layer instabilities from gliders. *J. Phys. Oceanogr.*, 46, 1285-1307.

Thorsos, E.I., F.S. Henyey, W.T. Elam, B.T. Hefner, S.A. Reynolds, and J. Yang (2010). Transport theory for shallow water propagation with rough boundaries, *AIP Conf. Proc*., 1272, 99–105, doi:10.1063/1.3493109.

Wang, X., J. Zhao, T. Hattermann, L. Lin, and P. Chen (2021). Transports and accumulations of Greenland Sea intermediate waters in the Norwegian Sea. *J. Geophys. Res. Oceans*, 126, doi:10.1029/2020JC016582.

Warner, J.C., B. Armstrong, R. He, and J. B. Zambon (2010). Development of a Coupled Ocean-Atmosphere-Wave-Sediment Transport (COAWST) modeling system. *Ocean Model.*, 35, 230–244.

Wenz, G.M. (1962). Acoustic ambient noise in the ocean: Spectra and sources. *J. Acoust. Soc. Am*., 34, 1936-1956, doi:10.1121/1.1909155.

Zedler, S.E., P.P. Niiler, D. Stammer, E. Terrill, and J. Morzel (2009). Ocean's response to Hurricane Frances and its implications for drag coefficient parameterization at high wind speeds. *J. Geophys. Res. Atmos*., 114, doi: 10.1029/2008JC005205.

REPORT DOCUMENTATION PAGE

Form Approved
OMB No. 0704-0188

1. REPORT DATE *(DD-MM-YYYY)*	2. REPORT TYPE	3. DATES COVERED *(From - To)*
13/01/2022	Technical Report	2021-2024

4. TITLE AND SUBTITLE
Northern Ocean Rapid Surface Evolution (NORSE):
Science and Experiment Plan

5a. CONTRACT NUMBER

5b. GRANT NUMBER
see report cover for complete list

5c. PROGRAM ELEMENT NUMBER

6. AUTHOR(S)
M. Ballard, J. MacKinnon, L. Rainville, H. Simmons, P. Abbot, K. Bergentz, A. Brakstad, L. Centurioni, J. Colosi, T. Duda, T. Farrar, I. Fer, L. Ferris, D. Gong, V. Hormann, S. Jayne, L. Johnson, C. Lee, D. Lucas, S. Merrifield, D. Olson, P.-M. Poulain, V. Premus, D. B. Reeder, E. Richards, A. Ruiz-Angulo, A. Savage, J. Shapiro, E. Skyllingstad, T. Spengler, J. Thomson, K. Våge, and K. Zeiden

5d. PROJECT NUMBER

5e. TASK NUMBER

5f. WORK UNIT NUMBER

7. PERFORMING ORGANIZATION NAME(S) AND ADDRESS(ES)
Applied Physics Laboratory - University of Washington
1013 NE 40th St.
Seattle, WA 98105

8. PERFORMING ORGANIZATION REPORT NUMBER
APL-UW TR 2102

9. SPONSORING/MONITORING AGENCY NAME(S) AND ADDRESS(ES)
Office of Naval Research
One Liberty Center
875 N. Randolph St., Suite 1425
Arlington, VA 22203

10. SPONSOR/MONITOR'S ACRONYM(S)

11. SPONSOR/MONITOR'S REPORT NUMBER(S)

12. DISTRIBUTION/AVAILABILITY STATEMENT
Approved for public release; distribution unlimited.

13. SUPPLEMENTARY NOTES

14. ABSTRACT
The NORSE DRI focuses on characterizing the key physical parameters and processes that govern the predictability of upper-ocean rapid evolution events occurring in the ice-free high latitudes. The goal is to identify which observable parameters are most influential in improving model predictability through inclusion by assimilation, and to field an autonomous observing network that optimizes sampling of high-priority fields. The overall goal is to demonstrate improvements in the predictability of the upper ocean physical fields associated with acoustic propagation over the course of the study. This Science Plan describes the specific objectives and implementation plan.

15. SUBJECT TERMS
Ocean variability; Acoustics; Ocean circulation; Fronts; Rapid changes; North Atlantic; Autonomous platforms

16. SECURITY CLASSIFICATION OF: a. REPORT	b. ABSTRACT	c. THIS PAGE	17. LIMITATION OF ABSTRACT	18. NUMBER OF PAGES	19a. NAME OF RESPONSIBLE PERSON
					Luc Rainville
					19b. TELEPHONE NUMBER *(Include area code)*
UNCL.	UNCL.	UNCL.	Unlimited	40	206 685 4058